



Thermochemical Characterization of Biomass

Modelling combustion and pyrolysis kinetic

Julia Garrigós Huelva

Thesis to obtain the Master of Science Degree in
Chemical Engineering

Supervisors: Prof. Francisco Manuel da Silva Lemos (IST), Luís António da Cruz
Tarelho (Universidade de Aveiro)

Examination Committee

Chairperson: Carlos Manuel Faria de Barros Henriques
Member of the Committee: Luís António da Cruz Tarelho
Member of the Committee: Moisés García Morales

November 2017

*“Nothing in life is to be feared,
it is only to be understood.
Now is the time to understand more,
so that we may fear less.”*

- Marie Curie

To Felix, for always being there, for not letting me give up and be my strength.

Acknowledgement:

First of all I would like to express my gratitude in a special way to Prof. Francisco Lemos and Prof. Maria Amélia Lemos, for their help, support and guidance, as well as for always having their doors open if I had any question.

I would like to thank as well to Prof. Moisés García Morales, who was my academic coordinator at the university of Huelva, for his efforts to help me in every problem I have had.

I would like to thank Mr. Everton Santos and Ms. Daniela Lopes Santos as well, for his kindness and his technical support in the laboratory and Mr. Hugo Pinto for his kindness in letting me use the equipment that he also needed to work.

Finally, all my thankfulness to my parents and my sister for their support and for believing in me. Without their help, I would have not been able to become an engineer.

Abstract

The current environmental situation faces serious problems of global warming. Thus, research, development and implementation of sustainable renewable energy sources is of vital importance. Of these technologies, biomass is one of the most attractive resources with a great potential for growth. However, for bioenergy technologies to be efficiently implemented, information is needed to estimate the cost of operation and maintenance of the biomass conversion processes. For this, it is indispensable to have information of the factors that affect the conversion of the biomass into energy.

In this project, it has been studied the kinetic of thermochemical conversion of five biomass samples, eucalyptus branch (ER), eucalyptus splinters (EA), eucalyptus bark (EC), eucalyptus pellets (EP) and acacia pellets (AP), under oxidizing and non-oxidizing atmospheres, and at different heating rates (10, 20, 50 and 100 °C/min). To do so, a thermogravimetric analyser (TGA) with differential scanning calorimetry (DSC) has been used to obtain the mass loss profile, mass loss rate and energy profile during the experiments. The biomass samples were prepared in collaboration with University of Aveiro and a pulp and paper company.

The data obtained allowed the estimation of the temperature range and the total mass loss of each of the stages that take place during pyrolysis and combustion, and the effect of the heating rate on those parameters. TG curves shown differentiated slopes that would correspond to the degradation of the different pseudo-components of biomass: water, cellulose, hemicellulose, lignin and ash. It was studied the conversion of each pseudo-component assuming a first-order reaction.

Finally, it has been studied the possibility to describe all the experiments with a single global reaction kinetics, that would predict the conversion of the samples during combustion and pyrolysis process for any heating rate.

Keywords: biomass, pyrolysis, combustion, kinetic of conversion, TG, DSC.

Resumo

A situação ambiental atual enfrenta graves problemas de aquecimento global. Assim, a pesquisa, desenvolvimento e implementação de fontes de energia renováveis sustentáveis é de vital importância. Destas tecnologias, a biomassa é um dos recursos mais atraentes com um grande potencial de crescimento. No entanto, para que as tecnologias de bioenergia sejam implementadas de forma eficiente, é necessária informação para estimar o custo de operação e manutenção dos processos de conversão de biomassa. Para isso, é indispensável ter informações sobre os fatores que afetam a conversão da biomassa em energia.

Neste estudo, estudou-se a cinética da conversão termoquímica de cinco amostras de biomassa, ramagem de eucalipto (ER), estilha de eucalipto (EA), casca de eucalipto (EC), pellets de eucalipto (EP) e pellets de acácia (AP), sob atmosferas oxidantes e não oxidantes e a diferentes taxas de aquecimento (10, 20, 50 e 100 °C / min). Para isso foi utilizado um analisador termogravimétrico (TGA) com calorimetria de varredura diferencial (DSC) para obter o perfil de perda de massa, taxa de perda de massa e perfil de energia durante os ensaios. As amostras de biomassa foram preparadas em colaboração com a Universidade de Aveiro e uma empresa da indústria da pasta e do papel.

Os dados obtidos permitem estimar a gama de temperaturas e a perda de massa total de cada uma das etapas que ocorrem durante a pirólise e a combustão, e o efeito das taxas de aquecimento nesses parâmetros. As curvas de TG apresentaram inclinações diferenciadas que corresponderiam à degradação dos diferentes pseudo-componentes da biomassa: água, celulose, hemicelulose, lignina e cinzas. Foi estudada a conversão de cada pseudo-componente assumindo uma reação de primeira ordem.

Finalmente, estudou-se a possibilidade de descrever todos os ensaios realizados com uma única cinética de reação global, que preveja a conversão das amostras durante a combustão e o processo de pirólise para qualquer taxa de aquecimento.

Palavras-Chave: biomassa, pirólise, combustão, cinética da conversão, TG, DSC.

Table of content

Abstract	4
Resumo.....	5
List of tables	7
List of figures	8
1. Introduction.....	9
1.1 Topic Overview	9
1.2 Objective.....	9
1.3 Problem statement. Bioenergy in the current energy situation.....	10
2. Theoretical Overview	12
2.1 Biomass.....	12
2.2 Composition of biomass	12
2.3 Biomass conversion processes	14
2.4 Process parameters	16
2.5 Review of macroscopic kinetic models	19
3. Experimental methods and equipment	26
3.1 Materials.....	26
3.2 Experimental method.....	26
3.3 Data processing	27
4. Experimental results.....	29
4.1 Analysis of thermal decomposition	29
4.2 Analysis of energy profile	31
4.3 Effect of the heating rate in mass loss profile.....	33
4.4 Effect of the heating rate in DSC curves.....	36
4.5 Model fitting.....	39
4.6 Kinetic parameters	40
5. Conclusion	50
References.....	52

List of tables

Table 1. Various Biomass feedstock	12
Table 2. Proportion of cellulose, hemicellulose and lignin in some lignocellulosic materials.	13
Table 3. Description of the samples and references	26
Table 4. Evaluation of mass loss and temperature peaks of each stages during combustion	30
Table 5. Evaluation of mass loss and temperature peaks of each stages during pyrolysis	31
Table 6. Exothermic peaks of all samples during combustion experiments at 10 °C/min	32
Table 7. Peaks of DTG curves during combustion for all samples at different heating rates	35
Table 8. Peaks of DTG curves during pyrolysis for all samples at different heating rates	35
Table 9. Temperature peaks in DSC curve for combustion at different heating rates.....	37
Table 10. Values of correlation coefficient (R^2) and the least-squares approach.....	40
Table 11. Statistical parameters of activation energy obtained at different heating rates	42
Table 12. Statistical parameters of activation energy obtained at different heating rates	45
Table 13. Fractions of biomass components obtained by the model during combustion.	47
Table 14. Fractions of biomass components obtained by the model during pyrolysis.	47

List of figures

Figure 1. Electricity power generation from solid biomass by region [4].	10
Figure 2. Structure of cellulose [12].	13
Figure 3. Structural organization of plant cell wall components. Source: [13].	14
Figure 4. Routes for biomass conversion and its products [1] [14].	15
Figure 5. TG and DTG curves of pyrolysis of wheat straw with different particle size	17
Figure 6. The volume fraction of the main gases obtained during pyrolysis of poplar wood	19
Figure 7. Design norms to maximize different products yields [1].	19
Figure 8. Structure of one component model [24].	20
Figure 9. Kilker and Broido 1965 [28].	20
Figure 10. Broido and Nelson, 1975 [30].	21
Figure 11. Shafizadeh and Bradbury, Bradbury et al, 1979 [29].	21
Figure 12. Chatterjee and Conrad, 1966 [32].	22
Figure 13. Koufopoulos et al, 1989 [33].	22
Figure 14. Shafizadeh and Chin, 1977.	22
Figure 15. Heating program for all samples	27
Figure 16. TG curves of combustion at a heating rate of 10 °C/min.	29
Figure 17. TG curves of pyrolysis at a heating rate of 10 °C/min.	30
Figure 18. Heat flow profile during combustion at a heating rate of 10 °C/min.	31
Figure 19. Heat flow profile during pyrolysis at a heating rate of 10 °C/min.	32
Figure 20. TG/DTG curves of samples during pyrolysis at different heating rates.	33
Figure 21. TG/DTG curves of samples during combustion at different heating rates.	34
Figure 22. DSC curves of combustion at different heating rates	36
Figure 23. DSC curves of pyrolysis at different heating rates.	38
Figure 24. Model fitting for combustion of all samples at 10 °C/min.	39
Figure 25. Apparent activation energies for all samples at different heating rates during combustion.	41
Figure 26. Apparent rate constant of dehydration stage for all samples at different heating rates.	43
Figure 27. Apparent rate constant for all samples at different heating rates.	43
Figure 28. Apparent activation energies for all samples at different heating rates during combustion.	44
Figure 29. Kinetic constant of first stage of pyrolysis.	45
Figure 30. Rate constants during pyrolysis at different heating rates.	46

1. Introduction

1.1 Topic Overview

Plants contain in their chemical structure molecules that store biochemical energy transformed from solar energy, in the presence of water and CO₂ through photosynthesis. The environmental benefits of its use as a source of energy are derived from the fact that the carbon contained in these molecules has been previously, and recently, captured from the atmosphere through photosynthesis, so the CO₂ released is not considered as a net increase in CO₂ concentrations in the atmosphere when the hydrocarbons present in these plants are used as fuel.

The utilization of this biochemical energy has motivated the research in the design of equipment and processes for the conversion of biomass, either through the biochemical or thermochemical routes, into usable fuels, as well as the study of the impact of the different types of biomass in this conversion. With the aim to optimise the conversion by thermochemical routes, it has been conducted kinetic studies to provide key information on the parameters that affect the reactions taking place both under air and under non-oxidative atmosphere.

The kinetics of the thermal conversion of the biomass will be considerably affected by its composition. *“Biomass is a complex mixture of organic materials such as carbohydrates, fats, and proteins, along with small amounts of minerals such as sodium, phosphorus, calcium, and iron”* [1]. However, we will be mostly interested in lignocellulosic materials and it can be considered that, for this type of biomass, the main components are hemicellulose, cellulose and lignin [2], natural polymers that form the structure of cell wall of plants, and as they degrade at different temperature ranges and rates, they will determine the overall reaction kinetics.

1.2 Objective

In this project a kinetic study of the thermochemical conversion of five different sources of solid biomass, eucalyptus branch (ER), eucalyptus splinters (EA), eucalyptus bark (EC), eucalyptus pellets (EP) and acacia pellets (AP) in different atmospheres and at different heating rates, was performed with the objective of characterizing the composition of the samples and provide information on the kinetic and thermal parameters of the main components that are involved in the thermochemical biomass conversion.

A final objective of the project was to determine whether it is possible to describe the experiments with a single global reaction kinetics which would predict accurately the kinetic behaviour of the samples when subjected to combustion and pyrolysis processes.

1.3 Problem statement. Bioenergy in the current energy situation.

There is a growing concern about the pollution of the environment caused by the human activities, in particular in what concerns carbon dioxide accumulation in the atmosphere. In this context, the use of biomass has been increasing in recent years as it can be seen in the figure 1, which represents the generation of global electric energy from solid biomass over the last 15 years, and where it can be seen a clearly growing trend. Also, the International Energy Agency (IEA) projects in its reports that this trend will continue to increase in the future, its estimations envisage world total primary bioenergy supply would increase from 50 EJ today to 160 EJ in 2050 [4].

Despite its tendency to increase, the contribution of bioenergy to world energy consumption nowadays is small; power generation from biomass represents 1.2% of total global power generation capacity and unfortunately, most of this bioenergy is associated with unsustainable biomass use, causing deforestation and soil degradation.

The countries with largest consumption of biomass for energy production are developing countries in Asia and Africa where the use of biomass is mostly for traditional cooking and heating. This traditional use of biomass implies very low conversion efficiencies, around 10% to 20%, and health damage issues through smoke pollution [3].

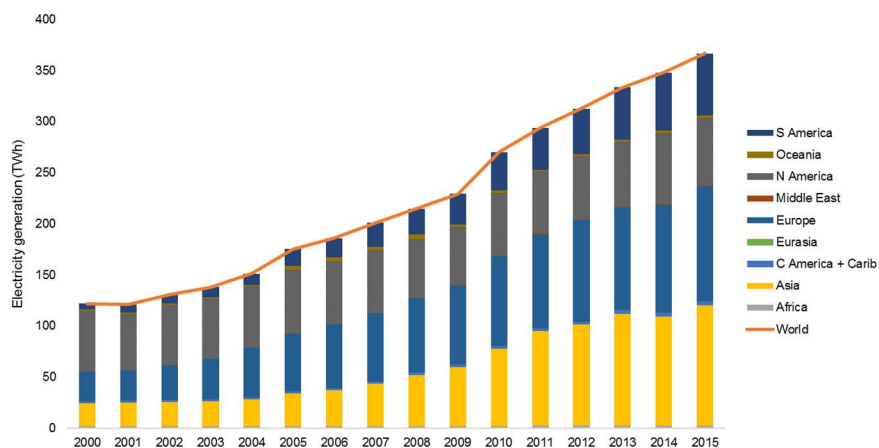


Figure 1. Electricity power generation from solid biomass by region [4].

In 2014 global electricity power generation from biomass represented about 8% of all renewable generation and around 1.4% to 1.5% of world electricity production. Electricity power generation from biomass is concentrated in OECD countries, where United States leads the global generation of electricity from biomass, followed by Germany and China [5] [6].

In the case of biofuels, the statistics show that biofuels provided around 4% (134 billion litres production) of world road transport fuel in 2015. Globally, United States and Brazil lead the biofuels producers ranking, where Ethanol is the main product. Other important producers are the European Union, Argentina and Indonesia, where Biodiesel is the main product [7].

One of the challenges facing the evolution of the bioenergy obtained through the use of solid biomass is the implementation of a criterion that ensures the sustainability and economic efficiency of its use. Key factors that assure the efficiency of the economics of different conversion routes are the moisture content, dry matter content and energy potential. Therefore, it is necessary to carry out lines of research that provide information about the reaction kinetics of the different biomass conversion routes.

2. Theoretical Overview

2.1 Biomass

The definition of Biomass established by the United Nations Framework Convention on Climate Change (UNFCCC) is the following;

“Biomass means non-fossilized and biodegradable organic material originating from plants, animals and micro-organisms. This shall also include products, by-products, residues and waste from agriculture, forestry and related industries as well as the non-fossilized and biodegradable organic fractions of industrial and municipal wastes. Biomass also includes gases and liquids recovered from the decomposition of non-fossilized and biodegradable organic material” [8].

Biomass feedstock characterization is an important factor to determine if it is feasible and profitable to use it as an energy source. According to the previous definition, it can clearly be seen that there is a large amount of organic material that can be classified as biomass due to its energy potential, and the sources to obtain it are very diverse. Based on the provenance of the biomass, it can be classified mainly in the following groups: agricultural residues, herbaceous crops, woody crops, forest residues and urban residues. Table 1 shows some of the most common examples of organic matter included in those groups.






<ul style="list-style-type: none"> • Corn stalks/stover • Sugarcane bagasse • Wheat straw • Hulls, shells, prunings • Fruit pits 	<ul style="list-style-type: none"> • Miscanthus • Switchgrass • Other grasses • Bamboo 	<ul style="list-style-type: none"> • Black locust • Eucalyptus • Hybrid poplar • Douglas fir • Poplar • Maple wood • Pine • Willow 	<ul style="list-style-type: none"> • Hardwood wood • Softwood wood 	<ul style="list-style-type: none"> • Municipal solid waste (MSW) • Refuse-derived fuel (RDF) • Newspaper • Corrugated paper • Waxed cartons
Agricultural Residues 	Herbaceous Crops 	Woody Crops 	Forest Residues 	Urban Residues 

Table 1. Various Biomass feedstock [5].

2.2 Composition of biomass

The structure of the biomass comprises mainly three components, the extractives, the cell wall and the ash. The extractives are fats, proteins, oil, starch and all those components that are present in minor proportion and that do not perform a structural function. The cell wall is a polymer mesh composed mainly of hemicellulose, cellulose and lignin, but also contains structural proteins, enzymes, phenolic polymers and other components that determine the chemical and physical characteristics of the cell wall. Ashes are the inorganic compounds present in the biomass. The composition of the biomass is a critical factor in determining the profitability of biomass power plants, since it will have an impact on the cost of the raw material, transportation and storage costs, and, thus, on the overall economy of the conversion process.

The proportion of hemicellulose, cellulose and lignin vary for different types of biomass. Table 2 shows typical proportions that have been determined for different feedstocks by some research studies.

Biomass	Hemicellulose (%)	Cellulose (%)	Lignin (%)
Rice straw	24	32.1	18
Sugar cane	25	42	20
Hardwood	24–40	40–55	18–25
Softwood	25–35	45-50	25–35
Deciduous	15-35	40-44	18-25
Coniferous	20-32	40-44	25-35
Willow	19	50	25
Larch	27	26	35
Corn stover	26	38	19
Newspaper	25–40	40–55	18–30
Grasses	25–50	25–40	10–30
Banana waste	14.8	13.2	14
<i>Eucalyptus saligna</i>	15	45	25
<i>Eucalyptus grummifera</i>	16	38	37

Table 2. Proportion of cellulose, hemicellulose and lignin in some lignocellulosic materials [1] [9] [10].

I. Cellulose

Cellulose ($C_6H_{10}O_5$)_n is an organic polymer made up of glucose bonded in its cyclic form β -D-glucopyranose by β -1,4-O-glycosidic bonds. The microfibrils of this polysaccharide form a structural element of the plant cell wall. Cellulose has a linear structure, without coiling or branching (Figure 2). Due to its functional groups, cellulose tends to form intermolecular and intramolecular hydrogen bonds, so it acquires a very rigid conformation that confers high tensile strength to the polysaccharide. This property is of great importance since it endows resistance to cell walls, where the microfibrils are interlaced forming the cellulose fibres [11].

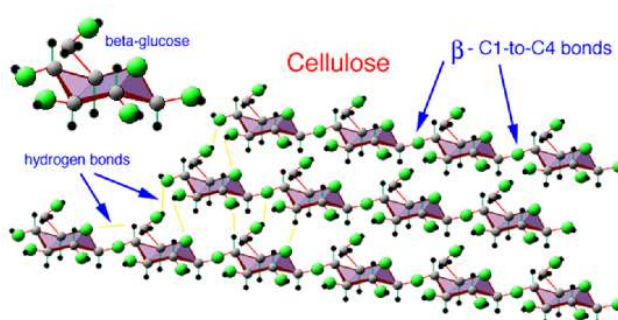


Figure 2. Structure of cellulose [12]

II. Hemicellulose

Hemicellulose ($C_5H_8O_4$)_n is a heterogeneous polysaccharide, that is it consists of the union of different types of polysaccharides, mainly D-xylose, L-arabinose, D-galactose, D-mannose, D- glucose and D- glucuronic acid. Since hemicellulose is composed of several types of carbohydrates, it is characterized

by having ramifications which cause the structure to be amorphous (Figure 3), which allows cellulose microfibrils and lignin hold together [1] [4].

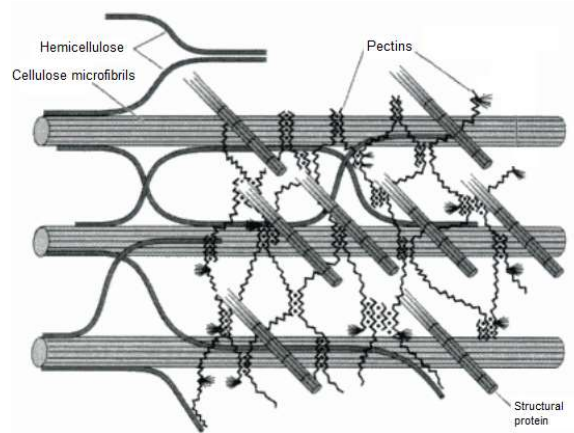


Figure 3. Structural organization of plant cell wall components. Source: [13].

III. Lignin

Lignin is a complex organic polymer with a three-dimensional and highly branched structure, consisting mainly of phenylpropanoid units, namely 4-propenyl phenol, 4-propenyl-2-methoxy phenol, and 4-propenyl-2,5-dimethoxy phenol [1]. The proportions of its constituents vary depending on the species, the organism or even the plant tissue of which it forms part [13].

2.3 Biomass conversion processes

Biomass can be converted through a variety of thermochemical processes, as combustion, gasification, pyrolysis, and liquefaction or through biochemical processes like anaerobic or aerobic digestion and fermentation. The thermal processes are those in which solid and dry biomass is subjected to high temperatures and in varying atmospheres of oxidation to release the chemical energy contained in the biomass and transform it into heat, mechanical energy or electricity or into different chemicals. Biochemical technologies use microorganisms or enzymes to break down the organic material into chemicals, including liquid and gaseous fuels as biogas, ethanol, methanol or biodiesel. Figure 4 summarizes the different technologies used for biomass conversion.

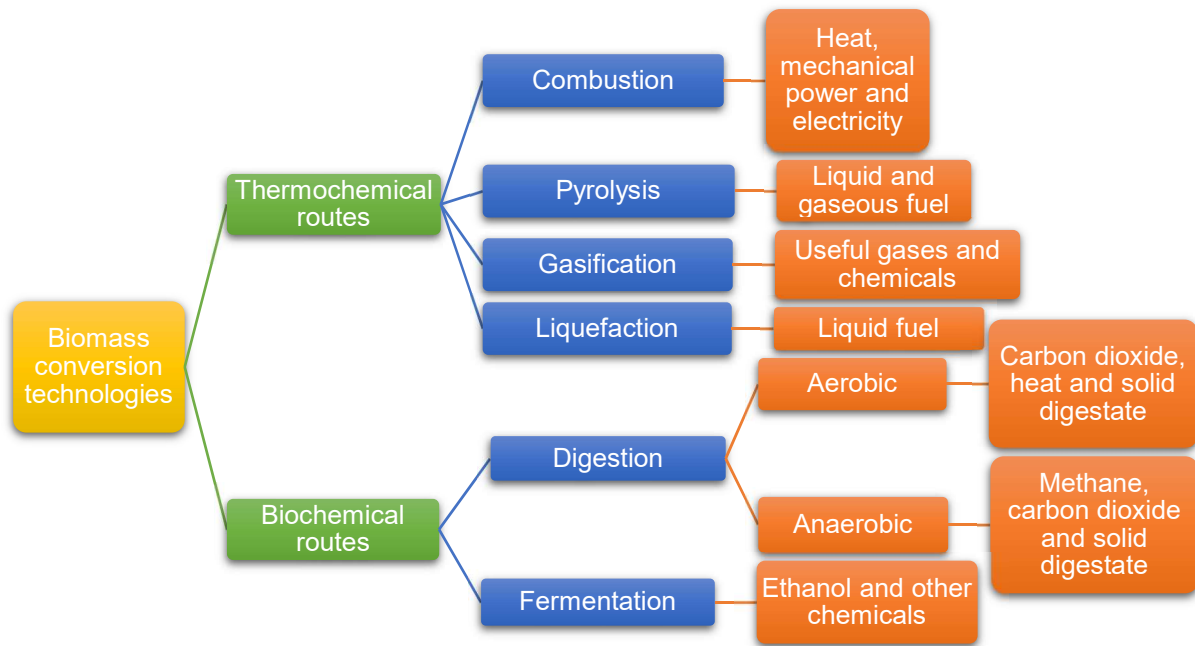
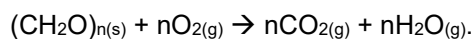


Figure 4. Routes for biomass conversion and its products [1] [14].

I. Combustion

Combustion is the process by which solid and partially dry biomass is subjected to high temperatures in an oxidizing atmosphere, with a sufficient amount of oxygen to ensure that the components are completely oxidized to gases, ash and residue. This reaction releases part of the internal energy of the fuel that manifests to the outside in the form of heat.

From the chemical point of view, combustion is an exothermic reaction between the oxygen and the hydrocarbons contained in the biomass, whose products are mainly CO₂ and H₂O. Although numerous intermediate reactions occur during the process, the process is usually presented by a single reaction:



During combustion, there is a first phase in which the sample is heated and releases the moisture it contains as well as low molecular weight gases such as CO and CO₂. When a temperature of about 250 °C is reached, the thermal decomposition of the components of the biomass begins [10]. In this stage, it is possible to differentiate two subsets, in which simultaneous and competitive reactions are carried out between them:

- **Volatilisation of the solid substrate and cracking** of the volatiles into smaller compounds.
- **Charring of volatiles.** This stage corresponds to flaming combustion, where the oxidation of the volatile compounds occurs.

The first step in the thermal decomposition of lignocellulosic biomass is the volatilisation of cellulose to levoglucosan, which is an endothermic reaction [10]. Then, there are numerous succeeding decompositions to lower molecular weight compounds that occur and that finally oxidise under flaming combustion. All these compounds reacting create a large number of intermediate products, some of them are even the products of secondary reactions occurring in gas phase between volatiles. Some of those intermediates are pentane, acetaldehyde, furan, and furfural [10]. The oxidation of these volatile components is an extremely fast and highly exothermic.

Apart from the reaction carried out in the gas phase, a heterogeneous solid-gas reaction also occurs upon the oxidation of the char through glowing combustion. It is a highly exothermic albeit slow process and requires high temperature conditions, around 700 °C for pure carbon [10].

II. Pyrolysis

Pyrolysis is the process of thermal degradation when samples are heated at high temperatures and in an inert atmosphere (total absence of oxygen). After an initial stage of drying, when the moisture is released, takes place an exothermic dehydration, when the inherent water and some low-molecular weight gases like CO and CO₂ are released. The next stage is the main devolatilization when the degradation of the long polymer chains of hemicellulose, cellulose and lignin occurs producing into char, condensable gases and non-condensable gases (CO, CO₂, H₂, CH₄) [1]. The last step would correspond to the carbonization of the volatiles and the degradation of the carbonaceous solid to produce char and noncondensable gases [15].

The degradation of lignocellulosic biomass is a complex process where reactions occur simultaneously to produce gaseous products as CO, CO₂, alcohols, aldehydes, acids, furan-ring products and anhydrosugars, and it produce also a char residue formed by fixed carbon and ash [16].

Depending on the type of pyrolysis that is used, the intermediate species formed during degradation of cellulose, hemicellulose and lignin can be cooled resulting in a dark liquid that contains many reactive species. This process is not exothermic, the interest in pyrolysis is due to that liquid product, a liquid fuel known as bio-oil, which stores the chemical energy contained in the biomass and its heating value is about a half of a conventional fuel oil [17]. Apart from fuel applications, valuable chemicals can also be extracted from the bio-oil.

2.4 Process parameters

Due to the great variety of parameters that affect biomass pyrolysis and biomass combustion, the process mechanism has become a complex puzzle that many researchers have tried to solve. Although there are a large number of research articles on biomass pyrolysis and combustion, the diversity of conditions and raw materials used to perform the experiments difficult the comparison of the results. The most important factors that affect the process are the physicochemical characteristics of biomass, the heating rate, the final temperature and the residence time in the reaction zone [1].

Physical and Chemical characteristics of Biomass

The generation and distribution of products will be conditioned by the physicochemical characteristics of the biomass, despite the operating conditions being the same [18], due to its effects on heat and mass transfer along the particle. One of the most influential factors in pyrolysis and combustion processes is particle size. A bigger particle size increases the resistance for the condensable gases to leave the particle, which favours the occurrence of secondary reactions between the volatile phase coming from the interior of the particle with the carbonized material that has already reacted on the surface of the particle [18]. Reversely, a finer particle size enables the movement of the primary products through the particle, which increase the liquid yields [1]. Primary pyrolysis releases CO₂, while secondary pyrolysis produce mainly CO and CH₄ [19].

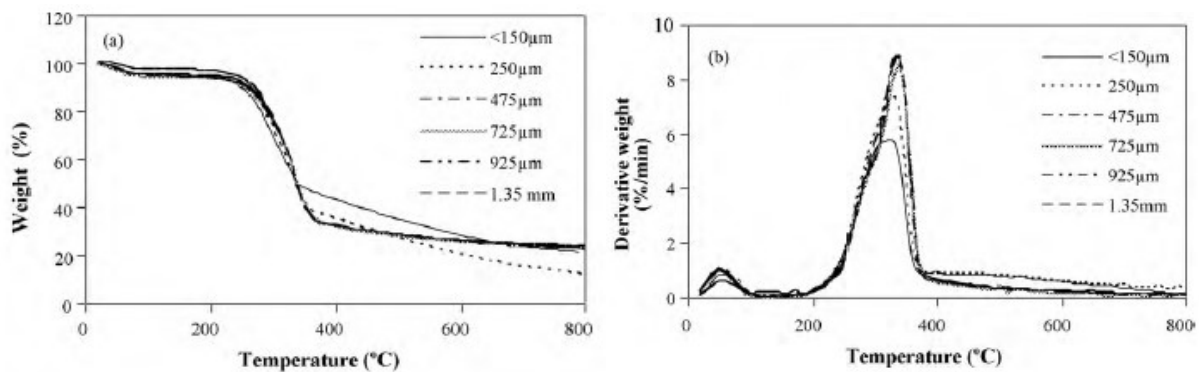


Figure 5. TG and DTG curves of pyrolysis of wheat straw with different particle size obtained by T. Mani, 2010 [20].

Because of the fact that particle size is a parameter that has been given great importance in the literature, many researches have been carried out with the aim of determining the effect of particle size on the thermal behaviour of biomass. Some of these studies often differentiate particles by size groups as for example Niemelä [21], whom separated the particles into three categories:

- Small particles (SF): 112-125 µm
- Medium particles (MF): 500-600 µm
- Large particles (LF): 800-1000 µm

Niemelä [21] has concluded that the thermal behaviour of the particles MF and LF is the same, whereas the behaviour of the SF deviates in the final stage of conversion curves and predicts a faster devolatilization. This result was also obtained by T. Mani [20] who studied the effect of particle size in the pyrolysis of wheat straw (Figure 5). The explanation proposed was that the kinetics of MF/LF particles incorporate the effects of internal heat transfer resistance, which means that kinetics can predict the thermal behaviour of particles, either medium or large, and that the effect of particle size can be considered negligible [22].

The composition of biomass is also an important factor, since it has a strong influence on the products of the process. The decomposition of the three major components of lignocellulosic biomass takes place in different temperature ranges and results in different products.

Yang [19] studied the decomposition of hemicellulose, cellulose and lignin in slow pyrolysis and determine the following temperature ranges:

- Hemicellulose: 220–315 °C
- Cellulose: 315–400 °C
- Lignin: 150–900 °C

Hemicellulose and cellulose decompose primarily into volatiles, hemicellulose in non-condensable gases (CO and CO₂), while cellulose in condensable gases. Lignin, on the other hand, decomposes primarily into char [1]. Therefore, the percentage in which this three major components are found in biomass influences the distribution of the products. The reason might be the different chemical structure of the components, in hemicelluloses there are more organic compounds with presents C=O groups, which generates more CO₂, cellulose shown higher contents of OH and C–O, which increase the release of CO, while there are more methoxyl–O–CH₃ groups in lignin, which produce more H₂ and CH₄ [19].

Effect of heating rate

The rate of heating is one of the most important factors in the process of pyrolysis and the combustion of biomass.

- High heating rates contribute to the formation of volatiles, and consequently to the production of liquid. Higher heating rates also favour the formation of temperature gradients inside the particle, which as mentioned above, promotes the appearance of secondary reactions, which results in a secondary char formation.
- Lower heating rates produce more char as it provides more contact time between the volatile phase and the solid phase.

Effect of final temperature

In the thermochemical conversion processes of biomass, the sample is heated to a final temperature. This final temperature affects the yield of the reaction and the composition of the products. Pyrolysis at high temperatures promotes the formation of the volatile phase, while low temperatures produce more char [1].

Figure 6 shows the different gaseous products yields obtained with different final temperatures during pyrolysis of poplar wood [23]. Increasing the final temperature favours the formation of non-condensable gases, because of the occurrence of secondary reactions. It also contributes to decrease the relative content of acids, which could be explained by the secondary degradation of acetic acid, while the content of phenols increase, which could be attributed to de degradation of lignin. Low final temperatures promotes the formation of solid products [23]. Figure 7 summarizes the contribution of the different parameters to each product yield.

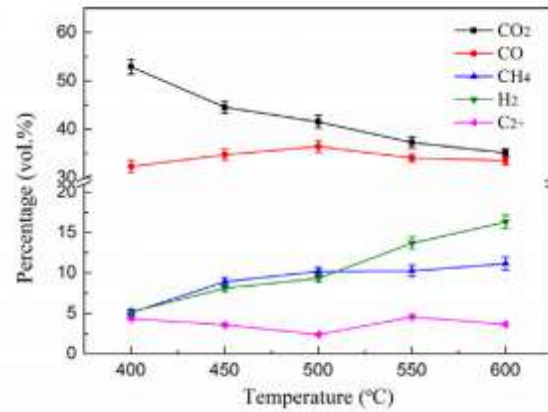


Figure 6. The volume fraction of the main gases obtained during pyrolysis of poplar wood under a heating rate of 30 °C/min (Source: Adapted from Chen, 2016 [23])

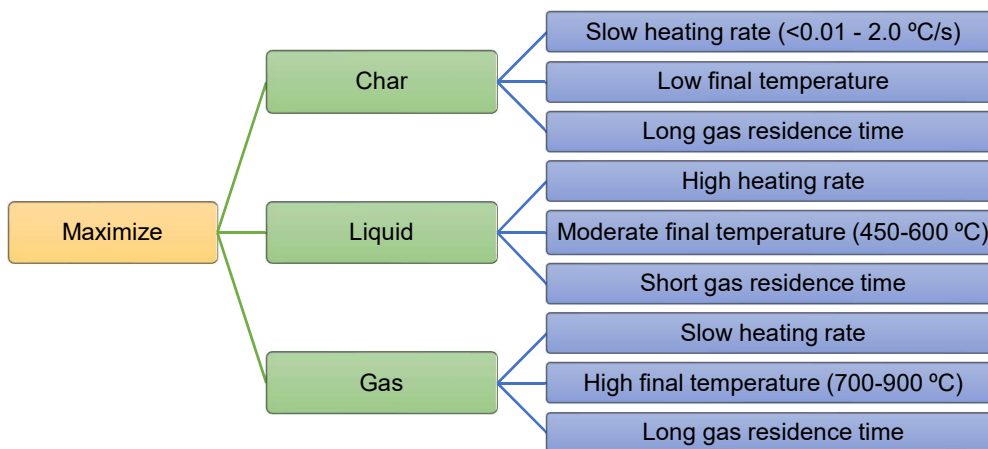


Figure 7. Design norms to maximize different products yields [1].

2.5 Review of macroscopic kinetic models

Thermochemical conversion of biomass, whether in an oxidizing or non-oxidizing atmosphere, involves multiple successive reactions, many of them competitive and extremely fast. Therefore, it is complicated to formulate a kinetic model that could predict the thermal behaviour of all the samples at molecular level. Thus, numerous studies have been carried out with the aim of formulating macroscopic kinetic models, from the simplest that considers a unique reaction of pseudo-first order, to models that consider three independent reactions assuming cellulose, hemicellulose and lignin as pseudocomponents and, at last, more detailed models considering numerous parallel, successive or competitive reactions. These models are mainly based on thermal behaviour simulation of the sample or product distribution and they usually focus on cellulose or woody biomass.

I. Models for pyrolysis product prediction

The lumped kinetic models describe biomass pyrolysis through one step or multi-step reactions that form tar, char and gases as products. A great variety of kinetic models has been proposed by different authors trying to approximate to the complexity of the real mechanism of biomass pyrolysis. The most widely used in research are explained below.

One step global models

One step global models were applied to the first experiments of biomass pyrolysis modelling. This model assumes a unique stage where the organic solid decomposes into volatiles and char with a fixed char yield through a first order reaction (Figure 8).

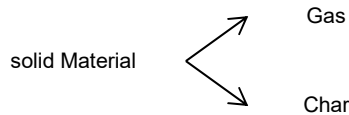


Figure 8. Structure of one component model [24].

Other authors have proposed models describing the pyrolysis of biomass through more complicated mechanisms, since the global reaction model does not allow to describe how hemicellulose, cellulose and lignin decompose in their own specific temperature range [25]. Vovelle [26] proposed in 1982 a model that would reflect the composition of wood as two groups of constituents: 50% of cellulose and 50% of secondary components (hemicellulose and lignin). Later in 1989, Varhegyi proposed a similar model using as raw material sugar cane bagasse [27]. His model consisted in two parallel reactions of first order, the first reaction is the decomposition of hemicellulose and the second reaction is the decomposition of cellulose. This model described in a mathematical way the theories proposed by Shafizadeh and McGinnis in 1971 that assumed that lignocellulosic biomass is composed of three main components (hemicellulose, cellulose and lignin) and that each component decomposes independently [2].

Multistep reaction models

The multiple reactions model considers parallel and competitive reactions or series reactions. The model describes a mechanism in which two reactions occur, dehydration, in which low-molecular-weight gases are released, and depolymerization, the phase in which volatiles are formed. From this model initially proposed by Kilker and Broido [28] new situations were proposed to simulate the real mechanism of pyrolysis, as the developed by Shafizadeh and Bradbury [29]. Some of the scenarios proposed in the literature are described below.

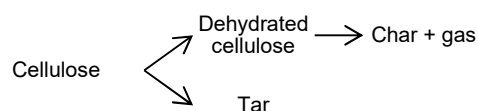


Figure 9. Kilker and Broido 1965 [28].

Model 1. Figure 9 represent a model that proposes three different processes during thermal degradation of cellulose. The first process is the dehydration of cellulose and it is an endothermic process. The second process would be the degradation of the cellulose to produce tar, primarily levoglucosan. This

process is also endothermic and competitive with the first process. Finally, an exothermic process would be the degradation of the “dehydrocellulose” releasing gas (CO, CO₂, H₂O, etc) and char [28].

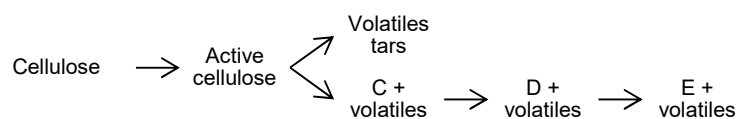


Figure 10. Broido and Nelson, 1975 [30].

Model 2. Broido and Nelson proposed the first model with the attempt to develop an approximation to calculate the kinetic parameters (Figure 10). They use the Arrhenius equation to relate the dependence of the temperature with the reaction constant. In this model, a first step is proposed in which cellulose reacts at high temperatures to form “active cellulose”, with a low degree of polymerization, and this active cellulose is degraded through two competitive mechanisms. The first is the degradation of the active cellulose to form volatiles, without char formation, and the second mechanism is constituted by a series of reactions that form solid intermediates C, D, and E in addition to volatiles [30]. Later, Varhegyi proved in a kinetic research that the decrease in the degree of polymerization of cellulose was not an limiting step in the mechanism of pyrolysis, so that step can be removed from the model [18].

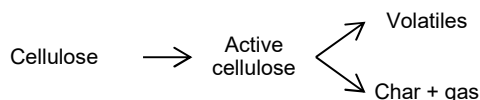


Figure 11. Shafizadeh and Bradbury, Bradbury et al, 1979 [29].

Model 3. Bradbury [29] proposed in 1979 a modification of the model developed by Broido [30], removing the series reactions D and E (Figure 11). It is known as Broido-Shafizadeh model and has been widely used in kinetic simulation. The model proposes a first endothermic stage, in which the degree of polymerization of cellulose is reduced, giving rise to an active cellulose. Then, two competitive reactions can occur, the first of which would be the degradation of this active cellulose to produce tar and the second one would be a slower and exothermic reaction that leads to the formation of gases (CO, CO₂, H₂O, etc) and char.

Broido [30] and Bradbury [29] calculated through the reaction rate equation of Arrhenius, the temperature at which the char formation rate is equal to the volatiles production rate and confirmed that

at low temperatures and with low heating rates, char production is favoured while tars production is favoured at high temperatures and with high heating rates [31].

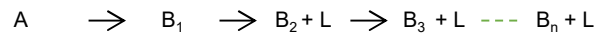


Figure 12. Chatterjee and Conrad, 1966 [32].

Model 4. In 1966 Chatterjee and Conrad [32] proposed a different approach to describe the pyrolysis of cellulose in a temperature range of 270-310 °C (Figure 12). His proposal was a mechanism of series reactions, in which there is a first stage where glucose bonds are broken down, and then depolymerization reactions occur giving rise to the formation of levoglucosan. This model was criticized for using a very reduce temperature range and for using a single heating program (3 K/min) [18].

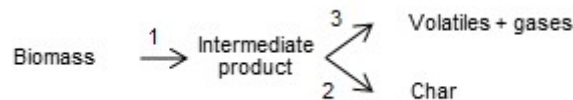


Figure 13. Koufopoulos et al, 1989 [33].

Model 5. Koufopoulos [33] proposed that biomass pyrolysis reaction rate its related with its composition and assumed that the total reaction rate can be considered as the sum of the reaction rates of the main components of biomass: hemicellulose, cellulose and lignin (Figure 13). In this way, the interactions between main components are considered to be negligible in the mechanism of biomass pyrolysis. The reactions rate is described with the Arrhenius equation. The model describes a first zero-order reaction that is not related with any weight loss. Then, the intermediate formed start to decompose through two competitive reactions (reaction 2 and 3). Reaction 2 produces char and reaction 3 produces gaseous/volatile products [24].

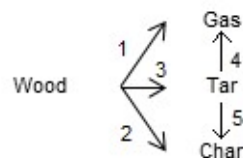


Figure 14. Shafizadeh and Chin, 1977.

Model 6. Figure 14 represent the model proposed by Shafizadeh and Chin (1977) for wood pyrolysis. The mechanism describes the decomposition of wood through three parallel reactions (reactions 1, 2,

and 3), called the primary reactions, to form tar, char and gases as products. Then, the tar decomposes through two parallel reactions (reactions 4 and 5), called the secondary reactions.

Comparison of kinetic models

Literature data has shown that thermal degradation of cellulose during pyrolysis could be well described by a first-order single step reaction model [31] [27]. However, one step global model does not describe the real mechanism of biomass pyrolysis and does not allow to estimate the correlation between product generation and reaction conditions [28] [34]. In addition, one step reaction models calculate the amount of volatiles produced by difference, so this mechanism does not provide information on the products distribution in condensable and non-condensable gases, char and tar [31]. Semi-global models are more interesting, since it is possible to estimate product distribution on relation to reaction conditions, since competitive reactions are included in the mechanism.

II. Macroscopic kinetic models for mass loss simulation

The macroscopic kinetic models most widely used to simulate the mass loss during biomass pyrolysis are the model-fitting method and the isoconversional method. The main objective of the simulation is to accurately and reliably calculate the apparent activation energy, the apparent reaction rate constant values and the reaction model $f(\alpha)$.

The rate of thermochemical conversion is often described in function of temperature as shown in Eq. (1).

$$\frac{d\alpha}{dt} = k(T) \cdot f(\alpha) \quad (1)$$

Where $k(T)$ is the reaction rate constant given by the Arrhenius equation and α is the conversion expressed as the fraction of the total mass-loss

$$k(T) = A \cdot e^{\left[\frac{-Ea}{R} \cdot \left(\frac{1}{T} - \frac{1}{T_{ref}} \right) \right]} \quad (2)$$

Where A is the apparent pre-exponential factor (min^{-1}), Ea is the apparent activation energy for the reaction ($\text{cal} \cdot \text{mol}^{-1}$), T is the temperature of the sample at every instant (K), T_{ref} is 300 K and R is the universal gas constant, $R=1.987$ ($\text{cal} \cdot \text{K}^{-1} \cdot \text{mol}^{-1}$).

Model-fitting method

Computational fitting methods are one of the most widely used methods in research. These methods assume a reaction model function $f(\alpha)$ and adjust the function with the experimental data through nonlinear least squares fitting to obtain the kinetic parameters [17]. The simulation of biomass pyrolysis as just one component reaction is not accurate enough, as already mentioned above. Thermal degradation of biomass is assumed to be the sum of the decomposition of its main pseudo-components: hemicellulose, cellulose and lignin [35].

The Kinetics Committee of the International Confederation for Thermal Analysis and Calorimetry (ICTAC) published recommendations in 2014 with the aim of improving kinetic analysis based on the experimental curves obtained by thermogravimetry techniques (TG), thermogravimetric analysis (TGA), differential scanning calorimetry (DSC), and differential thermal analysis (DTA). Among the recommendations mentioned it is included; the comparison of the experiments by at least three different heating rates, the quality of the fit should obtain a correlation coefficient (r^2) greater than 0.994 in the plot that compare the model with the experimental results, the use of an isoconversional method to verify the reliability of the calculated kinetic parameters and the validation of the rate expression with experimental data that have not been used to obtain the model [36].

Isoconversional methods

The isoconversional methods are one of the most accurate kinetic method to calculate parameters from thermochemical analysis. The method is based on the isoconversional principle that assumes that the reaction rate is a function that depend only in the temperature and its best property is that it is not necessary to assume a previous reaction model to calculate the kinetic parameters. It has been divided in the literature into its differential forms and its integral forms [37]. The differential form is expressed by the Friedman method, whose expression is shown in Eq. (3).

$$\ln \left(\frac{d\alpha}{dt} \right) = \ln(A \cdot f(\alpha)) - \frac{E}{RT} \quad (3)$$

The problem of the differential method is that thermogravimetric analysis result in a large amount of data, which produce high level of noise when differentiated. To avoid this problem, the integral method was proposed. The integral form of the equation is expressed in Eq. (4).

$$g(\alpha) = \int_0^\alpha \frac{A}{f(\alpha)} d\alpha = A \int_0^T e^{\left(\frac{-E}{RT}\right)} dT \quad (4)$$

The most used integral method is the one developed by Ozawa in 1965 [38] and Flynn and Wall in 1966 (FWO method) [39], who elaborate the following linear correlation to determine the kinetic parameter of biomass pyrolysis as a homogeneous single reaction.

$$\ln(\beta) = -1.0518 \cdot \left(\frac{E\alpha}{RT}\right) + \ln\left(\frac{AE\alpha}{Rg(\alpha)}\right) - 5,331 \quad (5)$$

Where β is the heating rate and $g(x)$ is a conversion function. By linearizing the equation, the kinetic parameters are obtained with the slope of the curve [40].

Another integral method is the Kissinger-Akahira-Sunose (KAS) method [41], proposed in order to obtain more precision than FWO method in the numerical integration, calculating the apparent activation energy by linear regression analysis. The Kissinger method is expressed in Eq. (6).

$$\ln \left(\frac{\beta}{T^2} \right) = \ln \left(\frac{AR}{E} \right) + \ln \left(\frac{1}{g(\alpha)} \right) - \frac{E}{RT} \quad (6)$$

The problem to use an integral method is to average the apparent activation energy which would cause errors in the calculation of the kinetic parameters during the numerical solution. Some advanced integral methods have solved this problem, for example the method of Vyazovkin [42], but its complexity cause the method to be very slow to run it computationally [43].

III. Conclusion of kinetic models

- Biomass pyrolysis can be described by three independent first order reactions, each reaction describing the individual thermal degradation of cellulose, hemicellulose and lignin as the pseudo components of lignocellulosic biomass [31] [27] [44].
- The reaction rate is well described by the Arrhenius equation [18].
- Lumped kinetic models are preliminary models since they provide a very slight information of biomass pyrolysis mechanism, focus only on estimation of char, tar and gases formation [40].
- Among isoconversional methods and model-fitting methods, model-fitting methods are the most extensively used since they are more easily implemented computationally. However, Isoconversional methods should be used to improve the accuracy of kinetic parameters when model-fitting methods are applied, as a complement to create a more solid and reliable procedure [40] [36].
- Model-fitting methods must be applied for more than three different heating programs and it would be interesting to validate the rate function with experimental data that have not been used to obtain the model [36].

3. Experimental methods and equipment

3.1 Materials

In this work a set of biomass samples, provide by a pulp and paper company, were investigated with the aim of characterizing their thermochemical behaviour under oxidative and non-oxidative conditions. The samples that were used in the study are presented in Table 3, together with the codes that will be used hereafter to designate them.

Sample	Code
Eucalyptus branch “ramagem de eucalipto”	ER
Eucalyptus pellets “pellets de eucalipto”	EP
Eucalyptus bark “casca de eucalito”	EC
Eucalyptus splinters “estilha de eucalipto”	EA
Acacia pellets “pellets de acácia”	AP

Table 3. Description of the samples and references

3.2 Experimental method

The experiments were carried out on a thermogravimetric analyser with a differential scanning calorimetry (STA 6000, PerkinElmer, Inc.) using an alumina crucible, for which the melting point is 2000 °C. As the maximum temperature reached is 800 °C there is no risk of melting the crucible.

Thermogravimetric analysis (TGA) measure the mass of the sample over time while the sample is subjected to a controlled heating program in a controlled atmosphere. This thermal analysis provide information of mass loss profile and rate of mass loss. The differential scanning calorimetry (DSC) provide information of the heat flow released or absorbed by the sample during the experiments.

To start all the experiments under uniform conditions and ensure a proper atmosphere within the equipment, a temperature of 30 °C is maintained for 30 minutes, then the equipment begins to heat the sample at the heating rate we indicate until reaching 800 °C, when the temperature is maintained for 5 minutes. Then, the equipment cools the sample from 800 °C to 30 °C at 50 °C / min. Experiments were carried-out under oxidative conditions, where the sweep gas was air, and non-oxidative conditions, using nitrogen, to obtain pyrolysis conditions. When pyrolysis was carried-out char was formed and thus, at the end of the first cycle, a second heating cycle was performed in an oxidative atmosphere to analyse the char that was formed.

To analyse the results of the experiments with different samples, and to ensure a greater accuracy, blank experiments were also conducted, using only the crucible, to observe if there is interference in the heat flow that can alter our results. Once the blank has been made, the experiments are carried out with the biomass samples. The initial weights of the samples were within the range of 20-30 mg. The experiments were performed at four different heating rates (10, 20, 50 and 100 °C / min) and in oxidizing and non-oxidizing atmospheres.

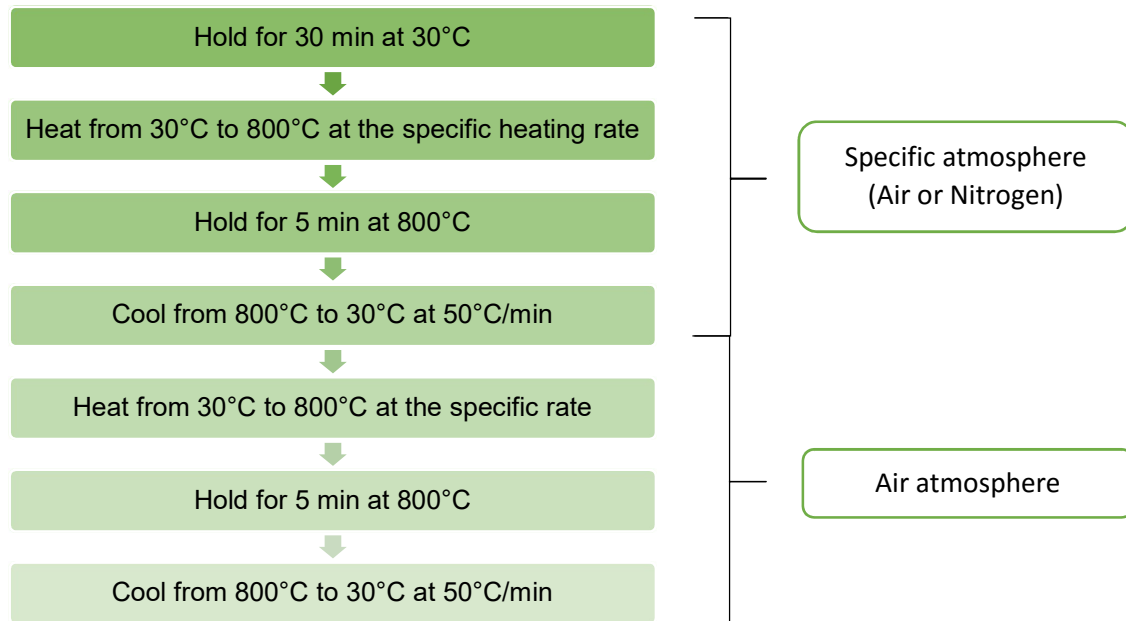


Figure 15. Heating program for all samples

3.3 Data processing

As it can be deduced from the review in section 2.5, there are numerous studies that search a kinetic model to estimate the thermochemical conversion of lignocellulosic materials, due to the interest in its use as an energy resource. However, there is a great variety of materials classified as biomass by its energy potential, and its conversion will be considerably affected by its composition, as already commented in section 2.4.

The procedure to calculate the kinetic parameters consist of the following steps:

- 4.1 The experiments are performed according to the experimental procedure indicated above and the data are loaded in an Excel file.
- 4.2 The weight fraction versus temperature is plotted on a graph and a kinetic model is computed in order to simulate the loss of experimental mass. In the context of this work we used a pseudo-component approach to describe the different biomass samples. The different pseudo-components can be tentatively assigned to the expected major components of biomass: water, cellulose, hemicellulose, lignin and ash.

It was assumed that the conversion of each pseudo-component follows a first-order reaction, which is, in a first approach, independent from the other pseudo-components. Thus, the kinetic model used to estimate the time-course evolution of the overall conversion describes the kinetics of each pseudo-component according to the expression,

$$-\frac{dW_{comp\ x,n}}{dt} = k(T) \cdot W_{comp\ x,n} \quad (7)$$

Where $k(T)$ is the reaction rate constant given by the Arrhenius equation Eq. (2) and $W_{comp\ x, n}$ represents the change in mass fraction of each individual pseudo-component at given time t_n and Δt is the time lap equal to 0.002 minutes. $W_{comp\ x, n}$ it is calculated by the Euler's method:

$$W_{comp\ x, n} = W_{comp\ x, (n-1)} + \frac{dW_{comp\ x, (n-1)}}{dt} \cdot \Delta t \quad (8)$$

4.3 The total modelled mass loss ($W_{model, n}$) it is calculated as the sum of the individual pseudo-components mass loss:

$$W_{model, n} = \sum W_{comp\ x, n} \quad (9)$$

4.4 The values of the activation energy, the pre-exponential factor and the initial mass fraction of each component, were estimated using a least-squares approach and resorting to the Generalized Reduced Gradient (GRG) algorithm for non-linear optimization using the Solver tool in Microsoft Excel.

The objective function to be minimized is, where $W_{exp, n}$ is the experimental mass loss.

$$f(W) = \sum (W_{exp, n} - W_{model, n})^2 \quad (10)$$

4. Experimental results

4.1 Analysis of thermal decomposition

Experiments performed on the TGA equipment provide us with information about the heat flow, absorbed or released by the sample during the test, as well as the variation of the sample weight. Representing the data of the weight variation of the samples with the temperature, it can be noticed that the slope of the mass variation curve differs at diverse temperature ranges (Figure 16).

I. Combustion

All the combustion experiments were carried-out under a flow of dry air of around 20 mL/min at normal temperature and pressure conditions, according to the temperature programme described in figure 15.

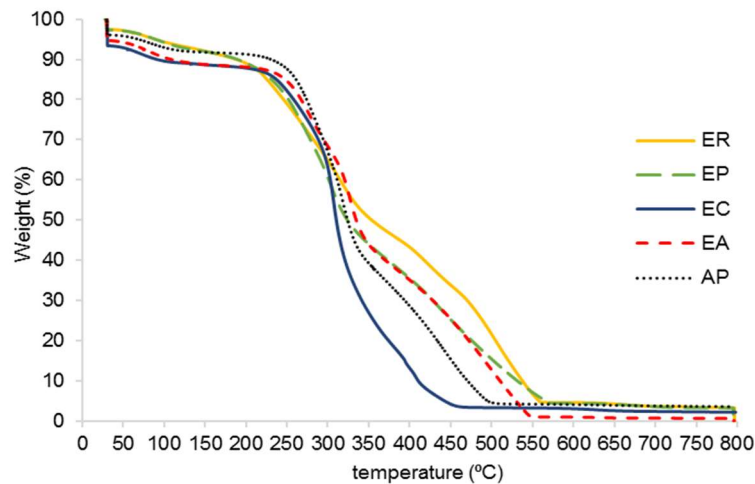


Figure 16. TG curves of combustion at a heating rate of 10 °C/min.

The first stage (30-140 °C), presents a small loss of mass, approximately 6-10% where the moisture contained in the sample and light-weight components are released.

The second stage (140-566 °C) corresponds to the combustion process and during it there is a high amount of mass loss, around 70-80%, when the volatilisation of the components of the sample and its cracking into smaller compounds occur. During this stage the oxidation of the volatiles may also occur. In this range of temperatures there is a first sub-stage (140-345 °C) where the rate of degradation increases and weight loss varies between 42-51% of the residual weight. The second sub-stage occurs at (345-566 °C), where the variation of weight oscillates between 31-48% of the residual weight.

The third stage (>566°C) correspond to the glowing combustion when the oxidation of the residual char takes place. In this stage, there is only a very small amount of mass loss, around 0,5-1%.

Table 4 indicates the more relevant parameters that were measured in these thermograms. The symbol "-“ indicates no peak found at that stage.

Sample	T _{stage 1}	Mass loss	T _{sub-stage 1}	Mass loss	T _{sub-stage 2}	Mass loss	T _{sub-stage 3}	Mass loss	T _{stage 3}	Mass loss	Ash
ER	116.88	6.62	-	-	339.28	41.62	555.35	48.29	555.65	0.05	3.42
EP	137.74	7.75	-	-	322.87	42.53	566.62	45.81	567.48	0.40	3.51
EC	74.74	8.67	272.21	12.58	345.29	36.91	646.08	38.93	653.11	0.02	2.89
EA	110.01	10.80	273.00	11.90	347.53	32.97	548.5	43.19	548.52	0.01	1.13
AP	167.4	8.36	-	-	344.36	50.97	488.37	34.38	672.47	2.35	3.90

Table 4. Evaluation of mass loss and temperature peaks of each stages during combustion at 10°C/min. Mass loss is expressed in percentages (%) and temperatures in Celsius (°C).

The fact that no peak had been found at the second substage indicate that the degradation of hemicellulose and cellulose occur almost simultaneously in the same substage.

II. Pyrolysis

The pyrolysis experiments were carried-out under a flow of dry nitrogen of around 20 mL/min at normal temperature and pressure conditions, according to the temperature programme described in figure 15.

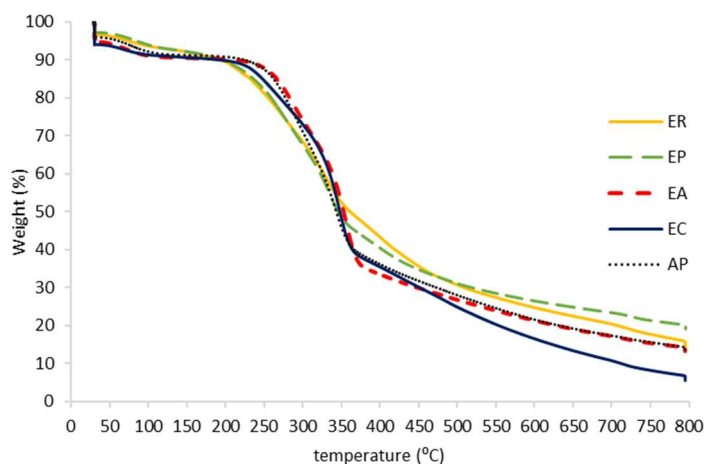


Figure 17. TG curves of pyrolysis at a heating rate of 10 °C/min.

Figure 17 shows a first stage (30-137 °C), that presents a small loss of mass, less than 10%, without alterations of the heat flow, where the moisture contained in the sample and light-weight components are released.

A second stage (137-795 °C) that corresponds to volatilization, where the degradation of the long polymer chains of hemicellulose, cellulose and lignin occurs to decompose into char, condensable gases and non-condensable gases. In this second stage, it is estimated that there is a first sub-stage that would correspond to the degradation of hemicellulose, since it has been observed to react at lower temperatures than cellulose or lignin, where the greatest variation in weight occurs between (220-315 °C [19]. In our case, the degradation of the first component, which is estimated to be hemicellulose, occurs at a higher temperature range (263-363 °C) with a weight loss varying between 4-18% of the

residual weight for the different samples. The second sub-stage (352-454 °C) would correspond to the degradation on cellulose, where the weight loss varies between 13-40% of the residual weight depending on the sample. Last, the degradation of the last component occur in a third sub-stage (497-795 °C) with a weight loss of 15-39% depending on the sample.

According to kinetic studies, cellulose degradation would occur in the temperature range (315-400 °C) and lignin degradation would occur slowly throughout the process until a temperature of 900 °C [19]. As It can be noticed, more ash is produced in pyrolysis process than in combustion since the volatilization of lignin, favoured at high temperatures during pyrolysis, produces a large amount of residue in the form of carbonaceous material along with ash, as already determined in previous studies [45]. The third stage would correspond to the carbonization of the volatiles and the carbonaceous solid.

Table 5 summarizes the data that was obtained. The symbol "-" indicates no peak found at that stage.

Sample	T _{stage 1}	Mass loss	T _{sub-stage 1}	Mass loss	T _{sub-stage 2}	Mass loss	T _{sub-stage 3}	Mass loss	T _{stage 3}	Mass loss	Ash
ER	124.55	7.15	363.69	43.29	453.77	14.40	688.85	14.25	750.44	3.20	17.71
EP	137.2	7.51	278.88	18.42	351.89	26.03	497.17	16.76	756	10.08	21.20
EC	109.8	8.89	263.38	9.54	354.27	36.50	795.13	39.40	-	-	5.67
EA	111.8	9.21	294.36	14.79	375.71	40.14	794.92	22.33	-	-	13.53
AP	115.3	8.44	288.24	15.78	357.05	33.14	794.22	28.79	-	-	13.85

Table 5. Evaluation of mass loss and temperature peaks of each stages during pyrolysis at 10°C/min. Mass loss is expressed in percentages (%) and temperatures in Celsius (°C).

4.2 Analysis of energy profile

In the following figures 18 and 19, the data of heat absorbed or released by the sample during combustion and pyrolysis at a heating rate of 10 °C/min are represented. Data were compared by temperatures, where it has been subtracted the thermal profile of the blank to eliminate the deviation produced by the crucible, and have been normalized with the weight of each sample to be compared.

I. Combustion

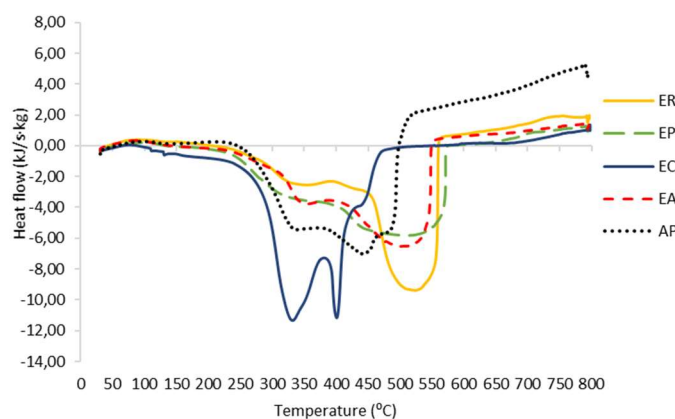


Figure 18. Heat flow profile during combustion at a heating rate of 10 °C/min.

The thermal profile shows an exothermic process at temperatures between (250-550 °C), and lightly endothermic at temperatures above 550 °C. Profiles of the samples follow a quite different behaviour from each other at temperatures below 550 °C, especially the eucalyptus bark (EC) sample, which peaks appear at lower temperatures than the other samples. At higher temperatures, the samples follow a similar behaviour, except acacia pellets (AP), which shows a more endothermal profile than the other samples. The main peaks are shown below (Table 6).

Sample	Peak (kJ/s·kg)	Temperature (°C)
ER	-2.54	354.43
	-9.39	523.6
EP	-3.92	399.99
	-5.82	510.6
EC	-11.34	331.94
	-11.17	401.05
EA	-3.77	355.93
	-6.53	498.84
AP	-5.44	338.68
	-7.02	442.09

Table 6. Exothermic peaks of all samples during combustion experiments at 10 °C/min

II. Pyrolysis

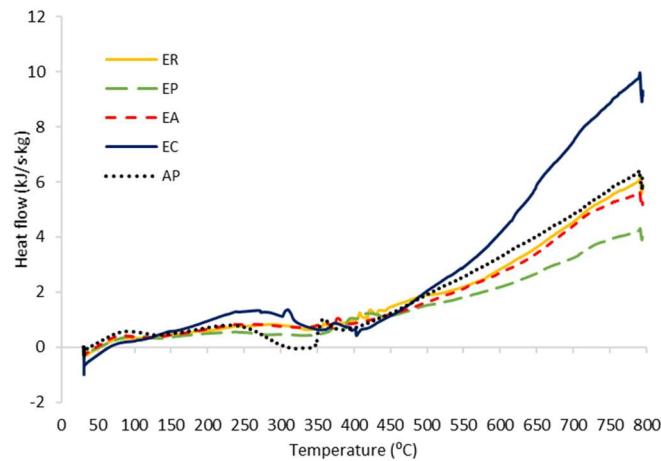


Figure 19. Heat flow profile during pyrolysis at a heating rate of 10 °C/min

The thermal profile of the samples when submitted to pyrolysis is completely endothermic. Despite the endothermic tendency, figure 19 shows how peaks and variations occur in the curve. As mentioned above, once the first dehydration stage occurs, volatilization of the components takes place, which is an endothermic process and at the same time it can occur the cracking of volatile phase already formed, which is an exothermic process [19]. The intermediate peaks and variations in the thermal profile that occur during the process may be since these two stages sometimes overlap, due to limitations in the heat transfer caused by the low thermal conductivity of the woody biomass [1].

4.3 Effect of the heating rate in mass loss profile

As commented before, the heating rate at which the sample is subjected during the experiments is one of the most influential parameters in the thermochemical conversion of the biomass. In this section, it is analysed the behaviour of each sample at different heating rates, to determine the effect of the heating rate in the mass loss profile and in the rate of mass loss.

I. Pyrolysis

TG curves of the samples at different heating rates (figure 20), show a similar behaviour at low temperatures, with small variations between them. As the temperature increases, the rate of mass loss decreases, which causes the stages to prolong and the slope become lower.

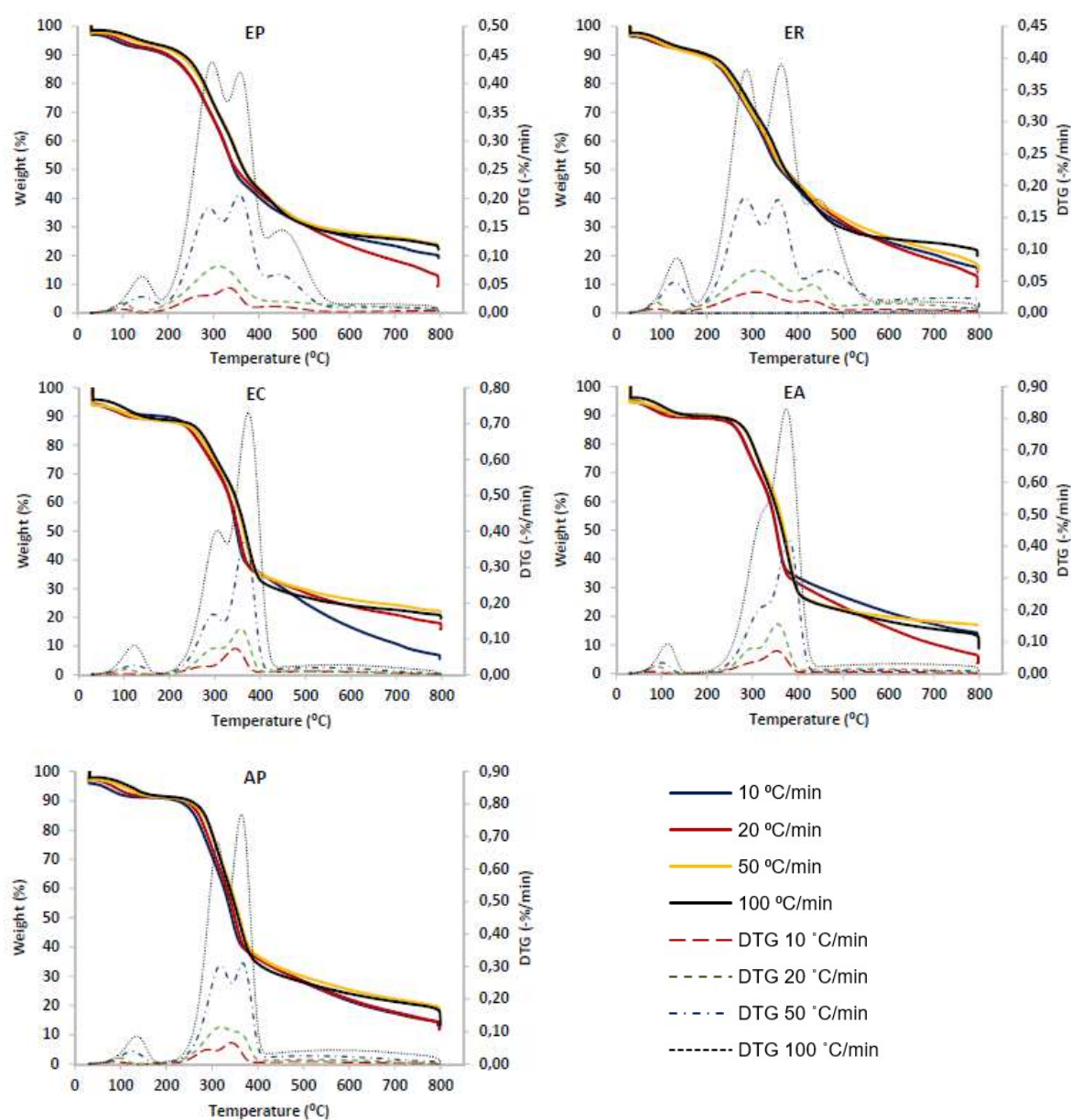


Figure 20. TG/DTG curves of samples during pyrolysis at different heating rates

II. Combustion

In the case of combustion, TG curves of the samples at different heating rates (figure 21), show the same behaviour as during pyrolysis, but at higher temperatures the difference between the slopes of the curves is higher than in pyrolysis.

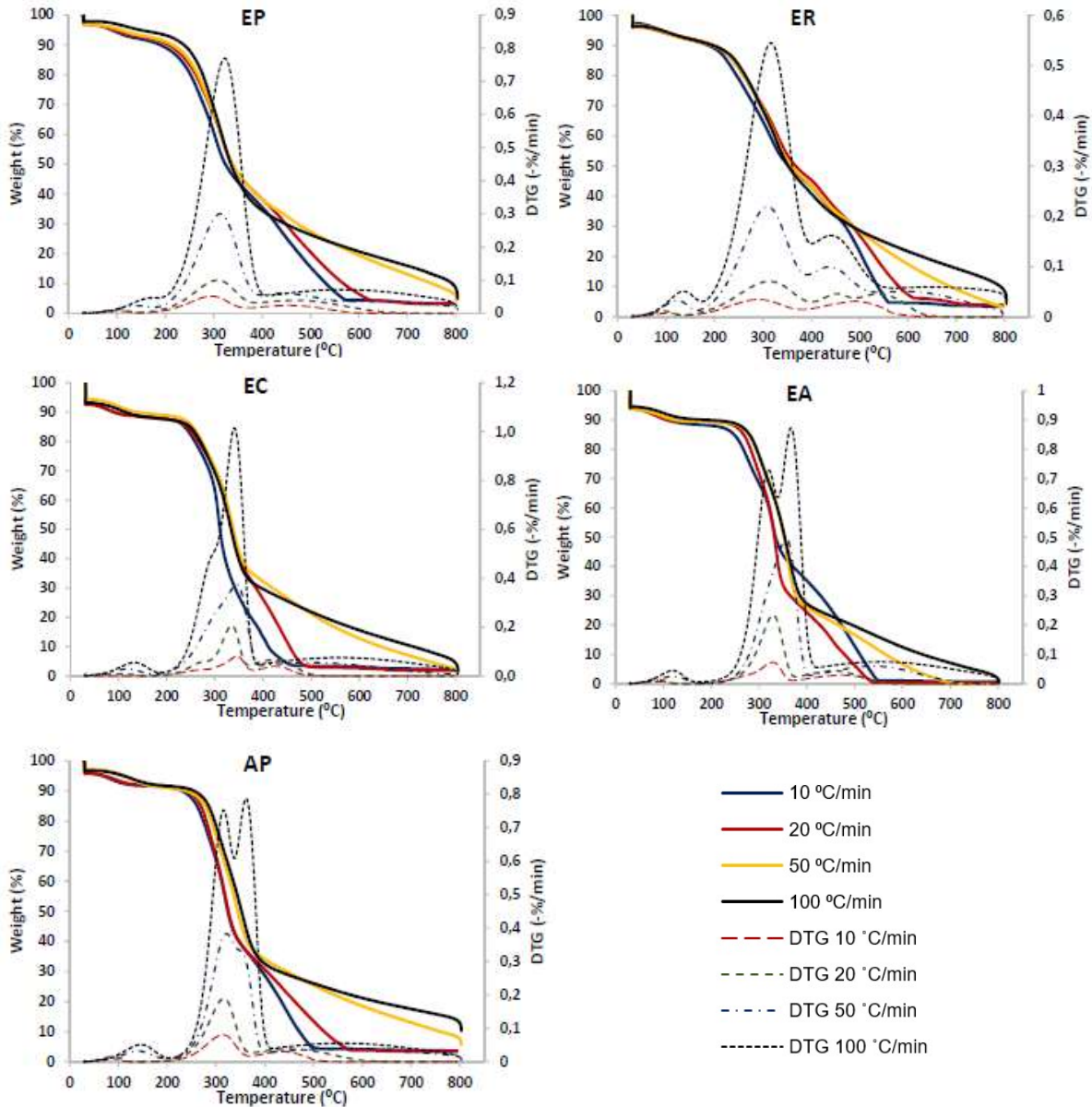


Figure 21. TG/DTG curves of samples during combustion at different heating rates.

Thus, increasing the heating rate causes the temperature range of the different stages to be larger and consequently the stages overlap. This may occur due to kinetic aspects or because although the heating rate has increased, there is a limitation in the heat transfer due to the thermal resistance of the sample [21]. A slower heating rate improves the heat transfer along the matter and ensures a more homogeneous temperature along the particle. As a consequence, the process of cracking is more efficient so more mass is reacting to form volatiles and the mass loss curve is deviated to produce less residue [20].

As for the rate of mass loss, the temperature at which the maximum weight variation is produced is displaced towards higher values. The reason might be that, as there is not an efficient heat transfer, a temperature gradient happens between the inner part and the surface of the particle, so the cracking occurs later than predicted if there was an efficient heat transfer [20].

Table 7 and Table 8 summarize the curve peaks of the rate of mass loss. The symbol “-“ indicates that no peak was found.

Sample		10 °C/min (°C)	20 °C/min (°C)	50 °C/min (°C)	100 °C/min (°C)
ER	Peak 1	101.1	95.21	122.51	135.84
	Peak 2	290.47	313.08	309.38	316.75
	Peak 3	491.36	452.87	437.39	440.68
EP	Peak 1	100.55	101.73	122.51	135.84
	Peak 2	295.3	307.51	312.88	322.25
EC	Peak1	90.28	103.98	119.54	132.61
	Peak 2	345.31	335.13	344.9	340.38
EA	Peak 1	90.6	85.23	120.73	119.47
	Peak 2	-	-	-	319.61
	Peak 3	328.43	329.3	356.74	366.79
AP	Peak 1	85.06	88.93	140.81	146.33
	Peak 2	-	-	-	315.67
	Peak 3	313.83	315.8	321.09	361.49

Table 7. Peaks of DTG curves during combustion for all samples at different heating rates

Sample		10 °C/min (°C)	20 °C/min (°C)	50 °C/min (°C)	100 °C/min (°C)
ER	Peak 1	88.26	87.37	128.66	133.85
	Peak 2	-	-	284.22	286.85
	Peak 3	305.72	309.06	356.24	363.02
	Peak 4	425.29	432.05	464.01	443.49
EP	Peak 1	97.09	100.7	141.99	142.81
	Peak 2	275.04	-	290.27	296.44
	Peak 3	333.87	311.18	356.89	358.28
	Peak 4	432.4	-	442.54	449.64
EC	Peak1	-	104.77	122.11	122.34
	Peak 2	253.67	293.37	296.23	305.18
	Peak 3	344.83	356.86	366.42	373.43
EA	Peak 1	-	89.67	100.97	113.12
	Peak 2	296.94	301.95	316.84	318.93
	Peak 3	353.24	355.4	379.27	374.78
AP	Peak 1	87.31	96.92	125.69	135.07
	Peak 2	291.3	319.16	318.38	311.91
	Peak 3	341.76	373.58	367.09	364.19

Table 8. Peaks of DTG curves during pyrolysis for all samples at different heating rates

4.4 Effect of the heating rate in DSC curves

I. Combustion

In this section, the results of the differential scanning calorimeter (DSC) are presented (Figure 22). The normalized heat flow curves are plotted as a function of the temperature of the samples. As it can be observed, all samples shows a similar heat flow profile. First there is an endothermic stage up to a temperature of 250 °C. This first stage would correspond to a dewatering stage, and the volatilization of low-molecular-weight gases. The second part of the process, which is exothermic, would correspond to the combustion of volatiles and, finally, char combustion. At temperatures above 500 °C in the case of the heating rate of 10°C/min, the heat flow profile shows a endothermic behaviour. The reason is that at this point, the combustion process has already been completed, and after that it may occur a volatilization of some minerals contained in the ash, generally potassium and sodium.

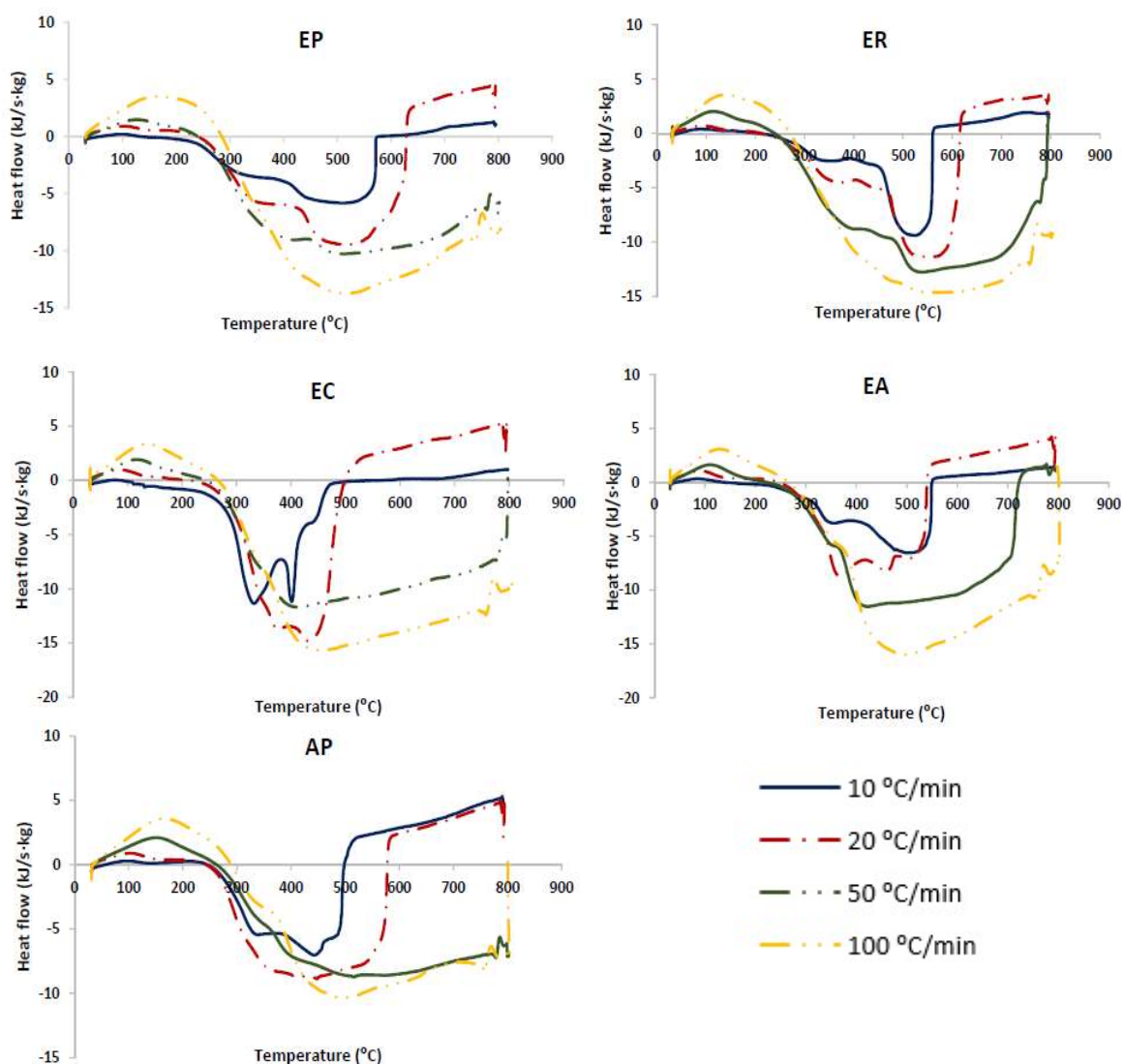


Figure 22. DSC curves of combustion at different heating rates

At low heating rates, generally two peaks can be seen, the first peak represents the combustion of volatiles, and the second peak represents the char combustion [46]. At higher heating rates, the peaks tend to approach each other so the heat flow profiles start to smooth out. Finally, at a heating rate of 100 °C/min, the two peaks are completely overlapped, and the curves show a single peak. This concurs with the heating rate effect that can be observed in TG curves in the previous section. As commented before, fast heating rates results in a temperature gradient along the particles which results in an overlap of the reactions. The combustion of volatiles and char are occurring almost simultaneously due to the temperature difference along the particle.

Table 9 summarizes the peaks of the DSC curve. The symbol “-” indicates that no peak was found.

Sample		10 °C/min (°C)	20 °C/min (°C)	50 °C/min (°C)	100 °C/min (°C)
ER	Peak 1	354.43	376.97	556.98	572.91
	Peak 2	523.6	553.5	-	-
EP	Peak 1	399.99	399.99	418.63	516.79
	Peak 2	510.6	517.3	510.51	-
EC	Peak 1	331.94	376.78	410.15	449.92
	Peak 2	401.05	429.31	-	-
EA	Peak 1	355.93	367.36	423.79	496.22
	Peak 2	498.84	456.11	-	-
AP	Peak 1	338.68	447.33	515.14	496.38
	Peak 2	442.09	-	-	-

Table 9. Temperature peaks in DSC curve for combustion at different heating rates

At higher heating rates, the temperature peaks, which as discussed above correspond to the combustion of volatiles and the combustion of char respectively, appear at higher temperatures. This effect can also be observed in DTG curves, and as already discussed, may be due to a temperature gradient between the inner part and the surface of the particle caused by the poor heat transfer.

As it can be seen in table 9, the sample which peaks appear earlier is the Eucalyptus bark (EC) followed by the acacia pellets (AP).

II. Pyrolysis

As can be seen in figure 23, the heat flow profile shows a completely endothermic behaviour at low heating rates, while at high heating rates, the DSC curve shows an exothermic behaviour at around 300-400 °C. The peaks seen in the heat flow would be related to the formation of the CO and CO₂ gases that occur simultaneously with the degradation of the sample [18].

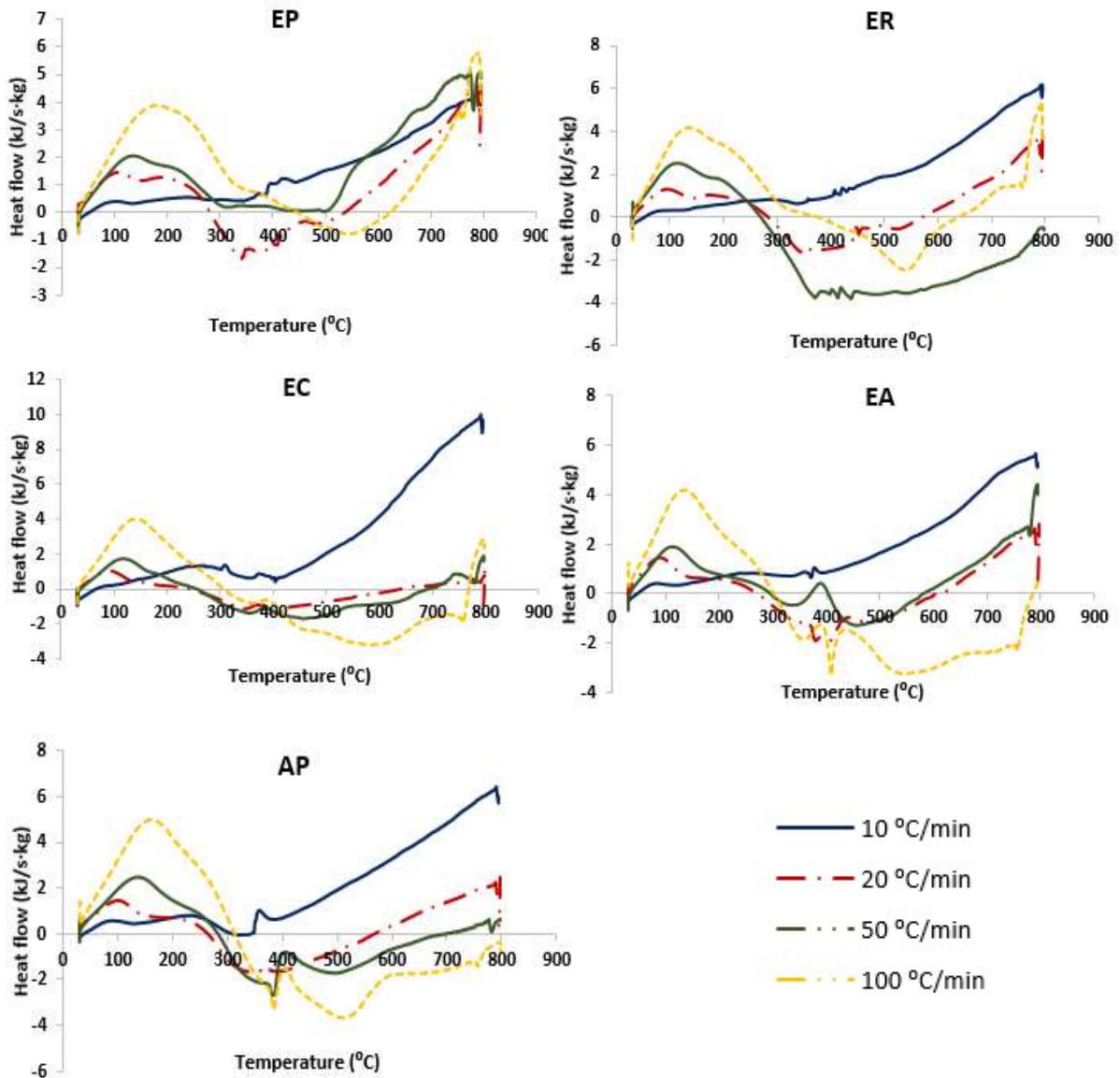


Figure 23. DSC curves of pyrolysis at different heating rates.

4.5 Model fitting

In this section, the graphs of model fitting for combustion of all samples at the rate of 10 °C/min are presented as representation of the models (figure 24), the values of the correlation coefficient (R^2) and the least-squares approach for the rest of the experiments are shown in table 10. These values show that the fitting of the curves is quite accurate, and the models can precisely describe the thermal behaviour of the samples.

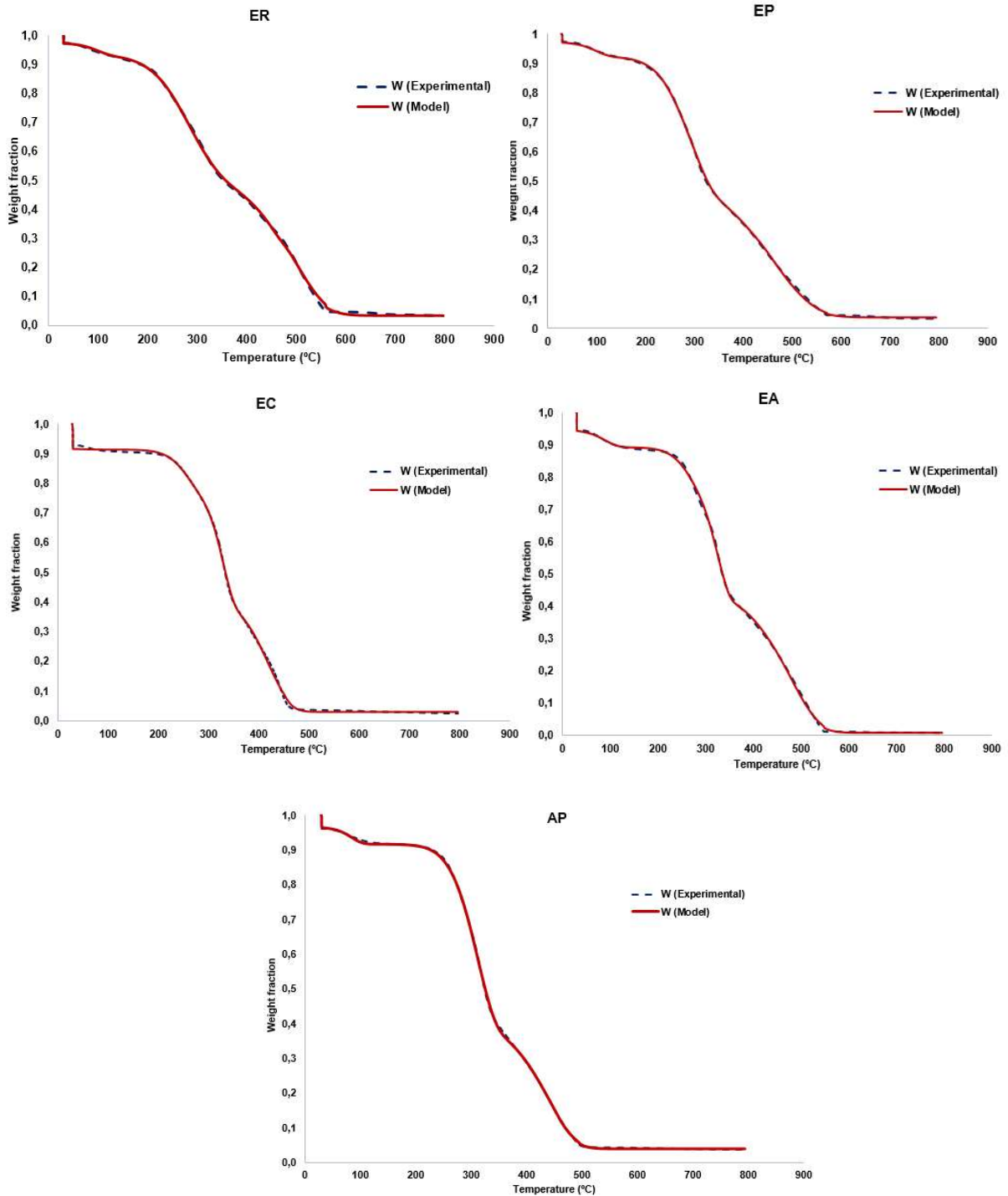


Figure 24. Model fitting for combustion of all samples at 10 °C/min.

Sample		10 °C/min		20 °C/min		50 °C/min		100 °C/min	
		R ²	f(W)	R ²	f(W)	R ²	f(W)	R ²	f(W)
ER	Combustion	0.9999	0.9699	0.9999	0.9611	0.9999	0.2694	0.9998	0.3846
	Pyrolysis	0.9996	2.0614	0.9997	1.0725	0.9999	0.2034	0.9998	0.1931
EP	Combustion	0.9999	0.7225	0.9999	0.3129	0.9999	0.3656	0.9998	0.1837
	Pyrolysis	0.9998	0.8154	0.9999	0.3675	0.9999	0.1470	0.9999	0.0914
EC	Combustion	0.9998	2.1104	0.9998	0.9526	0.9998	0.8766	0.9996	0.6193
	Pyrolysis	0.9998	1.4432	0.9997	1.2530	0.9997	0.536	0.9998	0.2994
EA	Combustion	0.9998	1.1689	0.9999	0.5926	0.9999	0.4550	0.9998	0.2252
	Pyrolysis	0.9998	1.0252	0.9999	0.5358	0.9998	0.4274	0.9999	0.2191
AP	Combustion	0.9992	0.9363	0.9999	0.6498	0.9999	0.6679	0.9998	0.2696
	Pyrolysis	0.9999	0.7111	0.9998	0.7589	0.9999	0.2068	0.9998	0.4594

Table 10. Values of correlation coefficient (R²) and the least-squares approach for all the experiments. f(W) represents regression function expressed in Eq (10).

It can be perceived that the experiments carried out at higher heating rates fit better to the experimental data than those performed at lower heating rates. This does not mean that the correlation between the model and the real mechanism are better described at higher heating rates, because as discussed above, at higher heating rates the heat transfer is not efficient and the reactions may overlap.

That is because, when using high heating rates, the final temperature is reached sooner, so the number of points that have been added to calculate the least-squares approximation is lower.

4.6 Kinetic parameters

The kinetic parameters estimated by the application of a multi-nonlinear regression model to the data are the activation energy E_a (kJ/mol) and the reaction rate constant, k (min⁻¹), as well as the apparent content of the main pseudocomponents in the samples.

I. Combustion

In Figure 25 are represented the apparent activation energy values obtained with the fitting model during combustion experiments at different heating rates (10, 20, 50 and 100 °C/min). The different apparent activation energies (E_a) can be tentatively assigned to the main pseudocomponents of biomass: water, cellulose, hemicellulose and lignin. " E_{aw} " would correspond to the activation energy of the water, since is the first component released during the process. Then, the next activation energies are successively assigned to the decomposition of hemicellulose, cellulose and finally lignin. The fourth component that appears in some experiments is related with the remaining lignin that is still degrading. It was added in order to improve the model fitting, as it was noticed that in some cases adding a new component reaction improve the quality of the model.

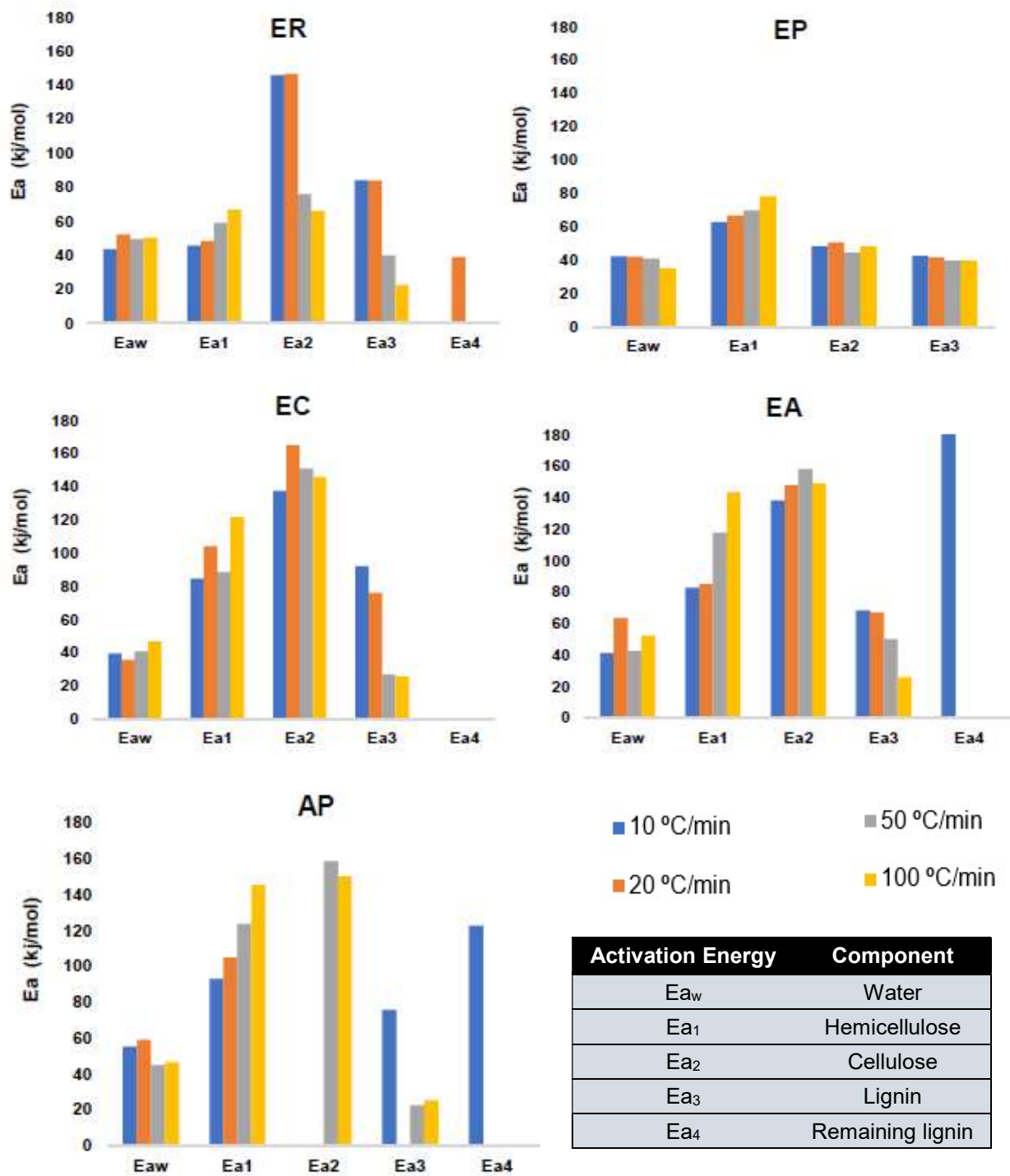


Figure 25. Apparent activation energies for all samples at different heating rates during combustion.

Sample	Parameter	Ea _{water} (kJ/mol)	Ea ₁ (kJ/mol)	Ea ₂ (kJ/mol)	Ea ₃ (kJ/mol)
ER	Ea	48.87	54.88	108.51	57.41
	σ	3.8	9.74	43.71	31.28
	CV	8%	0.18	0.4	0.54
EP	Ea	39.98	69.33	47.84	40.81
	σ	3.41	6.63	2.55	1.41
	CV	9%	0.1	0.05	0.03
EC	Ea	40.49	99.74	149.91	54.98
	σ	4.63	16.87	11.61	34.08
	CV	11%	0.17	0.08	0.62
EA	Ea	50.06	107.26	148.39	52.88
	σ	10.24	29.00	8.16	19.85
	CV	20%	0.27	0.06	0.38
AP	Ea	51.43	116.54	154.08	42.15
	σ	6.81	22.77	5.79	24.48
	CV	13%	0.2	0.04	0.58

Table 11. Statistical parameters of activation energy obtained at different heating rates during combustion. “Ea” is the apparent activation energy, “ σ ” is the standard deviation and “CV” is the coefficient of variation.

Standard deviation (σ) is a measure of data dispersion, it provides information of the distance between the data and the mean. The coefficient of variation (CV) represents the degree of variability of the sample, its value provides information of the reliability of the data.

Coefficient of Variation (CV):

- <10% → very acceptable (green)
- 10-20% → acceptable (orange)
- >20% → not reliable (red)

As it can be seen in table 11, the first stage, which corresponds to the loss of water and low-molecular-weight contained in the sample, remains stable for all samples, with a mean value of 46.17 kJ/mol and a coefficient of variation of 16%, taking into account all the samples at all heating rates. Also, it can be noticed that increasing the heating rate causes the activation energy of the first sub-stage to increase. As assumed above, this stage would correspond to the degradation of hemicellulose.

In the case of the second sub-stage, which would correspond to cellulose degradation, the values are more or less stable, the average value varies from 47.84 kJ/mol of the eucalyptus pellets (EP) to 154.08 kJ/mol of the acacia pellets (AP). The coefficients of variations are quite good for all the samples except the eucalyptus branch (ER), which indicates that the value of the apparent activation energy is not very reliable.

In the case of the last sub-stage, when degradation of lignin takes place, the difference between the values is higher. This was expected since TG curves at different heating rates shown similar behaviour at low temperatures, but the curves deviated significantly at higher temperatures. This, as commented before, may be due to the deflection in the measurement of temperature of the sample. The discrepancies may also arise from the fact that carbonization processes are significantly affected by the heating rate and this reaction is not adequately accounted for it. As a consequence, the coefficient of variation shows a high degree of variability between the data, which indicates that they are not reliable.

Below are shown the results of the apparent reaction rate for water in Figure 26 and for hemicellulose (k_1), cellulose (k_2), lignin (k_3) and the remaining lignin (k_4) in Figure 27.

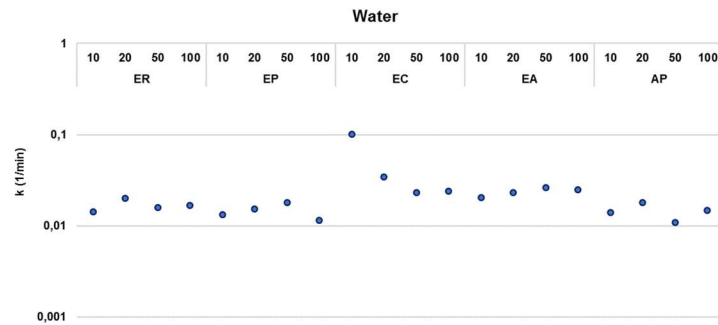


Figure 26. Apparent rate constant of dehydration stage for all samples at different heating rates.

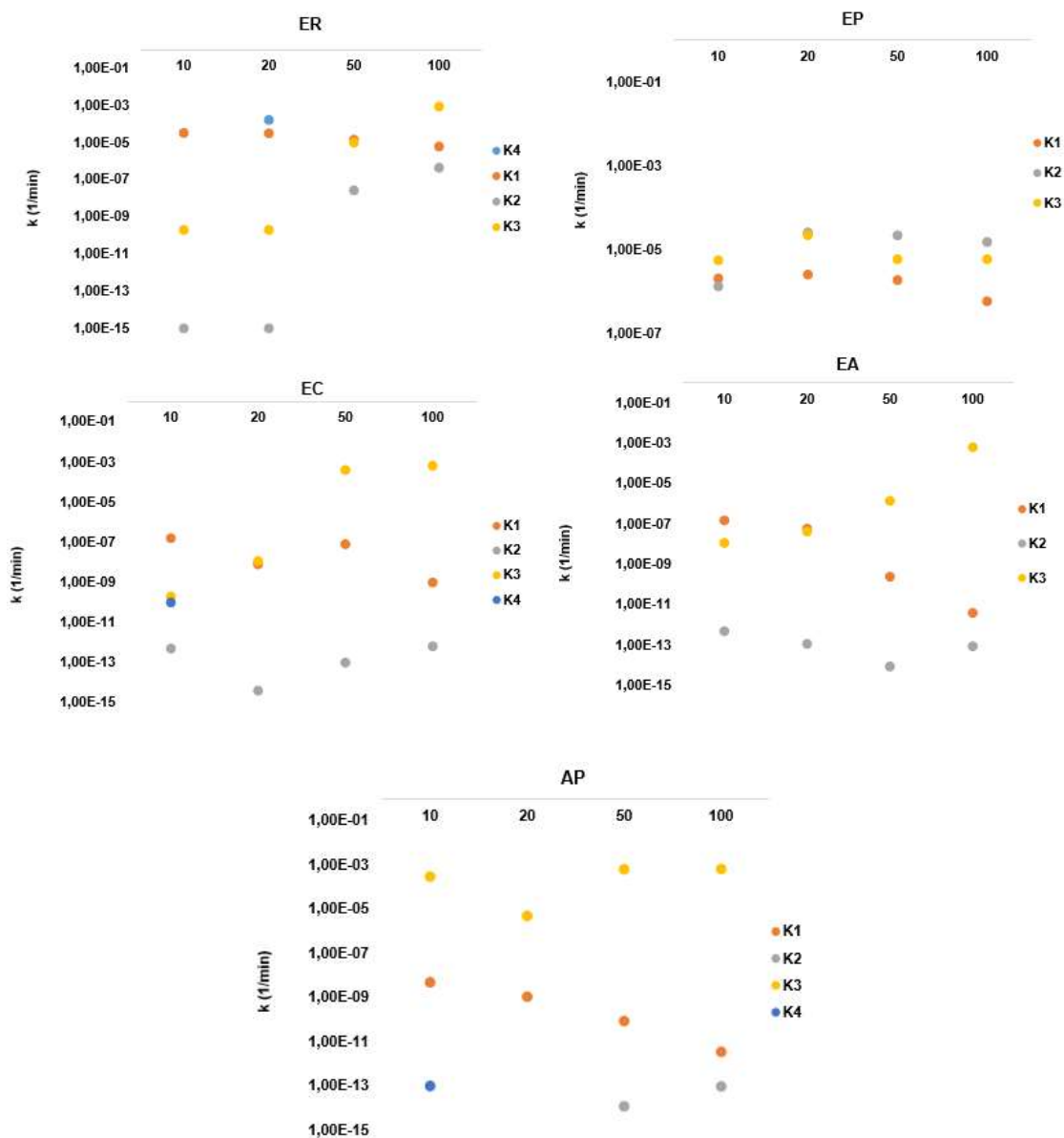


Figure 27. Apparent rate constant for all samples at different heating rates.

The rate constant " k_1 ", corresponding to the decomposition rate of hemicellulose, tends to decrease at higher heating rates while the constant " k_3 ", corresponding to the degradation of lignin, increases at higher heating rates.

II. Pyrolysis

In Figure 28 are represented the apparent activation energy values obtained with the fitting model during pyrolysis at different heating rates (10, 20, 50 and 100 °C/min).

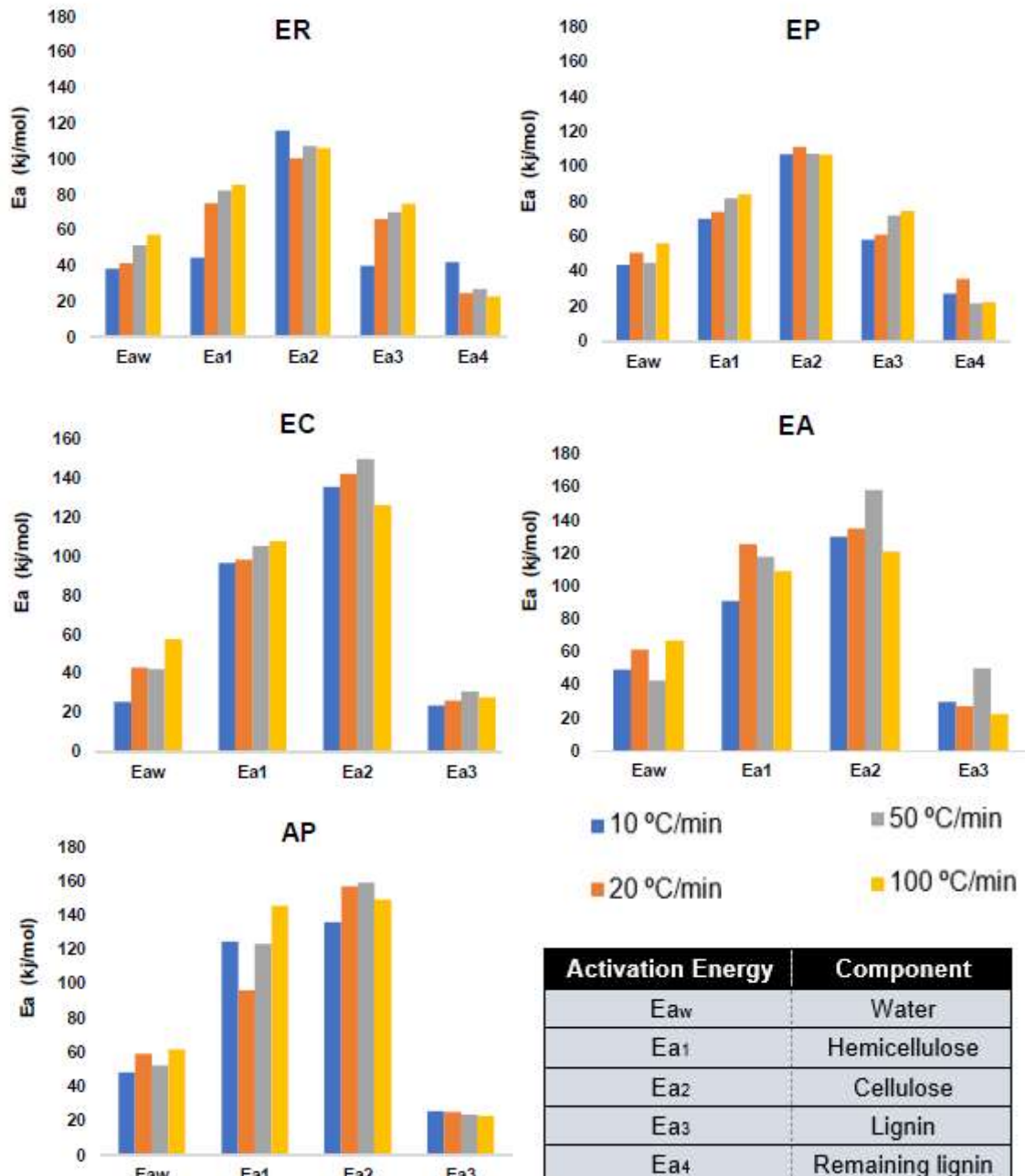


Figure 28. Apparent activation energies for all samples at different heating rates during combustion.

Sample	Parameter	Ea _{water} (kJ/mol)	Ea ₁ (kJ/mol)	Ea ₂ (kJ/mol)	Ea ₃ (kJ/mol)
ER	Ea	47.28	71.94	107.57	62.95
	σ	8.81	18.62	6.4	15.62
	CV	19%	0.26	0.06	0.25
EP	Ea	48.74	77.43	108.11	66.41
	σ	5.66	6.56	2.11	8.02
	CV	12%	0.08	0.02	0.12
EC	Ea	42.16	102.03	138.48	27.07
	σ	13.07	5.4	10.03	3.03
	CV	31%	0.05	0.07	0.11
EA	Ea	59.04	106.68	133.00	25.31
	σ	7.39	14.6	10.45	3.91
	CV	13%	0.14	0.08	0.15
AP	Ea	55.46	122.51	150.35	24.47
	σ	6.08	20.29	10.43	1.38
	CV	11%	0.17	0.07	0.06

Table 12. Statistical parameters of activation energy obtained at different heating rates during pyrolysis. "Ea" is the apparent activation energy, "σ" is the standard deviation and "CV" is the coefficient of variation.

As can be seen in table 12, pyrolysis results show better coefficients of variation (CV), which means that the values are closer in pyrolysis experiments than those of combustion at different heating rates. Almost all apparent activation energies are in the acceptable range of coefficients of variation.

The apparent activation energies obtained in the stages of dehydration and degradation of hemicellulose and cellulose are slightly higher in pyrolysis tests, whereas the last stage of lignin degradation the activation energies are lower in pyrolysis than in combustion. Despite the comparisons, the reactions that occur during pyrolysis and combustion are different, and therefore, the kinetic parameters will be different.

The kinetic constant of the dehydration stage increases with a higher heating rate, as expected since dehydration is an endothermic stage (Figure 29). The mean value is 0,016 min⁻¹ but it is highly variable because the model is very sensitive due to the fact that the samples have a low water content and varies for each sample.

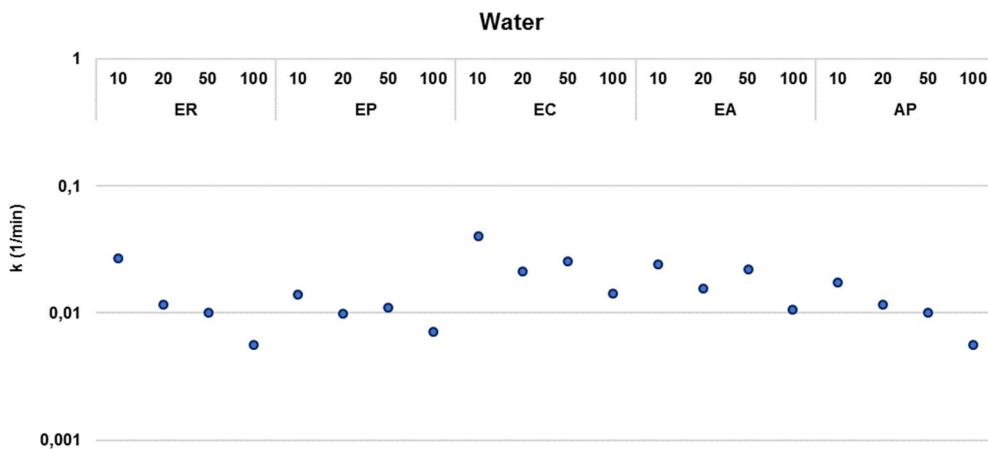


Figure 29. Kinetic constant of first stage of pyrolysis.

Figure 30 represents the results of the apparent reaction rate for hemicellulose (k_1), cellulose (k_2), lignin (k_3) and the remaining lignin (k_4) during pyrolysis obtained at different heating rates.

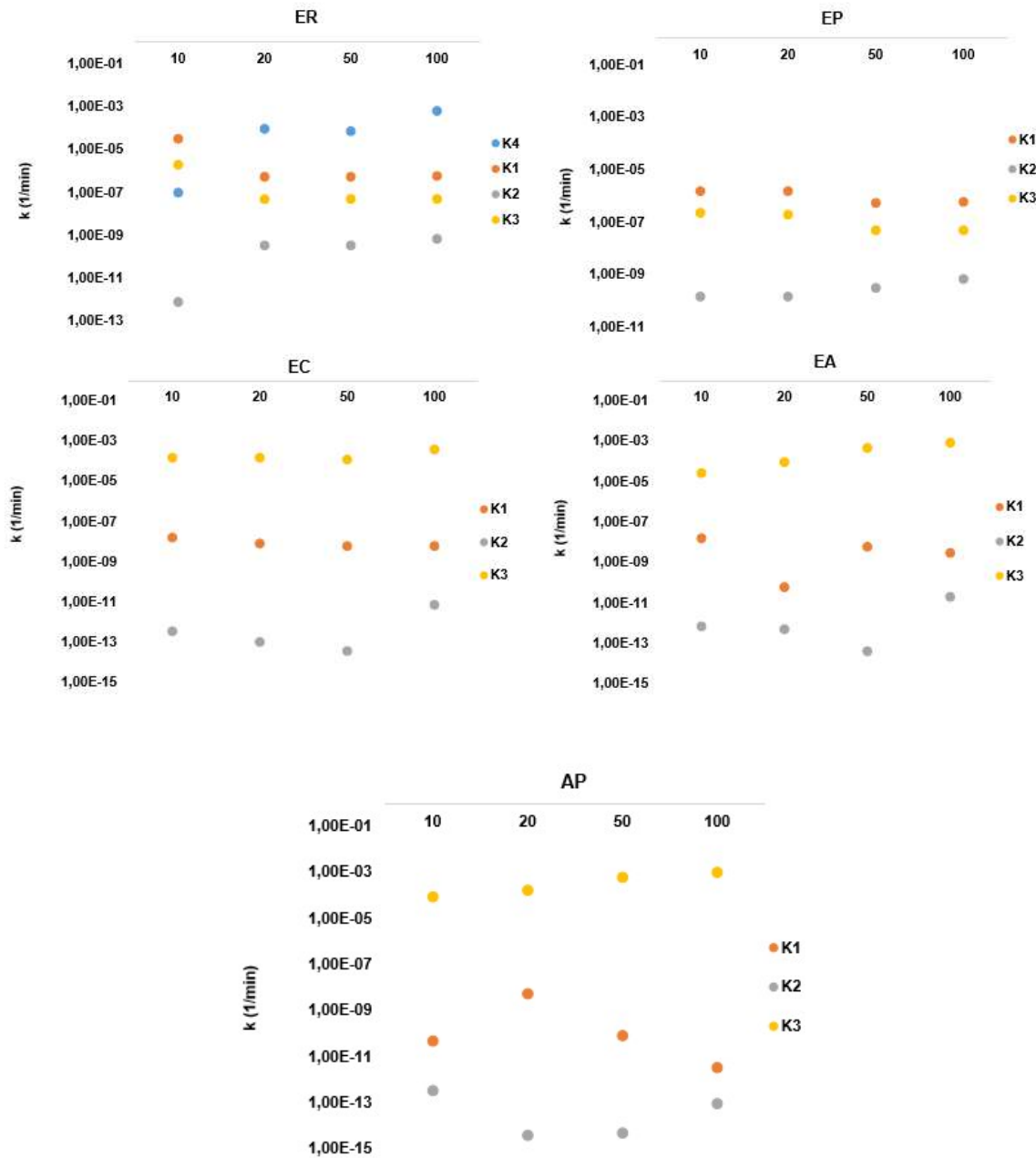


Figure 30. Rate constants during pyrolysis at different heating rates.

The rate constant " k_1 ", corresponding to the decomposition rate of hemicellulose, tends to decrease at higher heating rates while the constant " k_3 ", corresponding to the degradation of lignin, increases at higher heating rates. The rate constant " k_2 " corresponding to the decomposition of cellulose remains more or less constant. The difference in the final stage of the curves at different heating rates might be caused by the deflection in the measurement of the temperature, which produces a deviation in the kinetic parameters. The increment of the rate decomposition of hemicellulose, may be caused by the sensitivity of the fitting model, since the samples do not contain large amounts of water.

4.7 Biomass composition

Apart from the fitting of the apparent kinetic parameters, the model was also intended to provide estimates of the different fractions present in the samples. These were estimated from the experimental data for all the transformations. Table 13 and table 14 summarizes the data that was obtained. The symbol "-" indicates the fourth component reaction was not added.

Sample	Heating rate (°C/min)	W water (%)	W1 (%)	W2 (%)	W3 (%)	W4 (%)	W Ash (%)
ER	10	6.80	45.19	4.59	39.70	-	3.72
	20	6.60	33.46	9.17	33.29	13.11	4.37
	50	8.43	39.45	16.80	32.51	-	2.82
	100	7.09	42.86	14.88	32.00	-	3.18
EP	10	7.75	42.53	45.84	0.11	-	3.77
	20	6.61	40.39	49.29	0.47	-	3.24
	50	7.44	46.17	16.75	26.46	-	3.19
	100	8.00	53.26	13.34	24.01	-	5.03
EC	10	8.68	12.57	36.93	38.94	-	2.89
	20	11.78	11.89	35.05	39.05	-	2.22
	50	10.09	21.41	27.22	38.70	-	2.57
	100	11.62	13.31	41.06	31.64	-	2.38
EA	10	10.80	11.91	32.98	43.19	0.38	0.75
	20	10.32	15.47	41.55	32.34	-	0.33
	50	11.01	19.11	41.94	28.05	-	0.00
	100	8.91	21.95	38.34	30.36	-	0.44
AP	10	8.36	51.03	-	34.38	2.33	3.90
	20	8.00	49.51	-	39.21	-	3.28
	50	7.48	27.13	25.45	36.99	-	2.95
	100	7.60	23.25	34.29	23.21	-	11.66

Table 13. Fractions of biomass components obtained by the model during combustion.

Sample	Heating rate (°C/min)	W water (%)	W1 (%)	W2 (%)	W3 (%)	W4 (%)	W Ash (%)
ER	10	6.94	44.26	13.14	15.13	17.71	2.81
	20	9.39	24.64	16.33	11.85	32.06	5.72
	50	10.13	20.81	19.99	15.17	29.05	4.84
	100	8.78	20.67	20.75	19.71	10.31	19.77
EP	10	7.51	18.43	26.02	16.76	21.20	10.07
	20	7.43	18.79	24.63	16.79	25.16	7.20
	50	6.89	20.44	23.92	15.36	12.33	21.06
	100	6.21	22.97	23.55	16.22	9.22	21.83
EC	10	8.89	9.56	36.51	39.40	-	5.65
	20	11.05	17.74	32.60	21.35	-	17.26
	50	11.24	16.02	36.98	13.75	-	22.01
	100	10.59	16.48	41.86	11.00	-	20.07
EA	10	9.21	14.80	40.14	22.38	-	13.47
	20	10.41	13.19	41.02	31.25	-	4.14
	50	9.62	18.70	46.16	12.03	-	13.49
	100	9.36	15.74	48.65	17.06	-	9.18
AP	10	8.53	15.86	33.07	28.66	-	13.88
	20	7.77	30.35	20.65	27.73	-	13.50
	50	7.86	24.43	27.76	21.41	-	18.53
	100	7.34	21.84	34.73	20.79	-	15.30

Table 14. Fractions of biomass components obtained by the model during pyrolysis.

Eucalyptus is widely used in the manufacture of paper pulp and its residues are bark, branches and sawdust among others. Bark is the external layer of the trunk and it is formed by an outer dead part and an inner live part. Hemicellulose content is higher in inner parts of the trunk and lignin content is higher in outer parts of the trunk. However, cellulose is the mayor component of lignocellulosic biomass.

Water:

It can be seen from the tables 13 and 14 that the water content is low, less than 12% for all samples. The samples with the highest water content are Eucalyptus bark (EB) and Eucalyptus splinters (EA) with an average water content of 10.50% and 9.95% respectively, which agrees with the research carried out by Chen [47] about the thermal behaviour of some Eucalyptus residues, which attributes a greater water content in the bark (EC) of 10.89%.

The samples with lower water content are the Eucalyptus branches (EB) with 7.35% of average content, Eucalyptus pellets (EP) with 7.23% and acacia pellets (AP) with 7.87%. The water content is consistent with what is expected since the pellets are designed to be compact and have a low water content to make transport and storage more economical and efficient. Even so, the low amount of water in the samples causes a minor sensitivity of the model and therefore no accurate data can be provided on the amount of water.

Hemicellulose:

The sample with the lowest amount of hemicellulose is the Eucalyptus Bark (EC) with an average value of 12% taking into account the data obtained in both pyrolysis and combustion tests. The next sample with a slightly higher content of hemicellulose is the Eucalyptus splinters (EA) with a value around 16%. The samples with the highest hemicellulose content, around 30%, are the Eucalyptus pellets (EP) and acacia pellets (AP), and lastly the highest percentage of hemicellulose, around 35%, appear in the Eucalyptus branch (ER).

The hemicellulose content in the samples agrees with the analysis carried out by Chen [47] whom reported in his research a content of 12.90% hemicellulose in the eucalyptus bark (EC) and with Heidari [48] whom reported a hemicellulose content in Eucalyptus wood of 13.49%. However, the content of hemicellulose shown great variability, due to the low content of water which, as commented before, affect the sensibility of the model, so the content of hemicellulose cannot be accurately calculated if a dry basis is not used.

Cellulose:

Cellulose content was higher in the samples of eucalyptus bark (EC) and splinters (EA), with an average content of 36.03% and 41.35% respectively, both data with a coefficient of variation of 13% and 11 %, which means that the data are reliable. The samples of acacia pellets (AP) also shown a high content of cellulose, around 29.32%, their coefficient variation is in the acceptable range.

The samples of eucalyptus pellets (EP) show a content around 27.92%, and finally, the sample with the lowest cellulose content is the eucalyptus branch (ER) with a value around 17.71%, these data show great variation, therefore they are not reliable.

Chen [47] also reported higher content of cellulose in Eucalyptus splinters (33.89%), than in eucalyptus bark (27.48%), although his analysis shown a lower amount of both components. Heidari [48] determined a higher cellulose content in eucalyptus wood of around 46.25%.

Lignin:

Lignin content is highly variable since lignin decomposes over a wide temperature range, and it is the last of the three main pseudocomponents of biomass to degrade. As the temperature in the process increases, the heating rate begins to affect the heat and mass transfer processes, which causes the last stage to advance through different reaction mechanisms.

What can be deduced from the data is that at lower heating rates, there is a more efficient heat transfer, which leads to more efficient degradation of the pseudocomponents and less residue formation.

The average value obtained from lignin in all samples is about 20% during pyrolysis and 30% during the combustion. Eucalyptus pellets (EP) and eucalyptus branches (ER) are the samples that shown the least amount of lignin with an average of 16% during the pyrolysis. Chen [47] determined a lignin content of 32.09% for eucalyptus bark, 20.77% for eucalyptus sawdust and 9.25% for eucalyptus leaves and Heidari [48] found an average of 34% of lignin in eucalyptus wood.

5. Conclusion

Finally, it is going to be presented a summary of the main theme that have been developed in this thesis, remarking briefly the main objective of the thesis and the experimental results.

The main objective of this thesis is to study the thermal behaviour of five different samples of biomass, eucalyptus branch (ER), eucalyptus splinters (EA), eucalyptus bark (EC), eucalyptus pellets (EP) and acacia pellets (AP) under oxidizing and non-oxidizing atmospheres and at four different heating rates (10, 20, 50 and 100 °C/min).

The information sought to be obtained with this project are the kinetic parameters involved in the pyrolysis and combustion reactions of each one of the samples as well as the effect of the heating rate in the evolution of the reaction mechanism, as well as estimates of the composition of the samples.

To calculate the kinetic parameters, a fitting model has been employed to simulate the mass loss as a function of temperature, using a least-squares approach and resorting to the Generalized Reduced Gradient (GRG) algorithm for non-linear optimization using the Solver tool in Microsoft Excel.

Based on the mass loss profile, it can be determined that the thermal degradation of the samples can be well described by three independent first order reactions, that would correspond to the individual thermal degradation of cellulose, hemicellulose and lignin as the pseudo-components of lignocellulosic biomass, since the experimental results shown a very good correlation ($r^2 > 0.99$) for both combustion and pyrolysis tests.

The evolution of weight loss shown that at higher heating rates the temperature range of the different process stages widen causing the overlapping of the stages. Literature explain this effect as a consequence of a limitation in the heat transfer due to thermal resistance of the particles. Lower heating rates improve the heat transport and avoid temperature gradients along the particle. As a consequence, the cracking stage is more efficient because more matter is reacting to form volatiles and less residue is generated.

At low heating rates, generally two peaks can be seen, the first peak represents the combustion of volatiles, and the second peak represents the char combustion. At higher heating rates, the peaks tend to approach each other so the heat flow profiles start to smooth out. At a heating rate of 100 °C/min, the two peaks are completely overlap, and the curves show an unique peak.

Concerning kinetic parameters, the data obtained in the first stage of hemicellulose degradation show great variability, this stage can be affected by the sensitivity of the model during the dehydration stage due to the low amount of water in the samples.

The apparent activation energies of cellulose obtained by the model show a quite reliable coefficients of variation (<10%). The apparent activation energies have been slightly higher in the combustion tests than in the pyrolysis tests. Except in the case of the eucalyptus branch (ER), which shows the opposite and, also, the difference between the activation energies is especially large, 47.84 kJ/mol was obtained

during the combustion experiments, and 108.11 kJ/mol during pyrolysis. The apparent activation energy obtained during pyrolysis is more consistent with the data from the other samples, which vary between 107-154 kJ / mol. This may be due to a different reaction pathway that have taken place during the combustion.

Results indicate that cellulose has a higher activation energy than hemicellulose and lignin, so cellulose has a rapid conversion at fast heating rates. During combustion, the rate constant of hemicellulose decomposition tends to decrease at higher heating rates, while the rate constant of lignin degradation increase at higher heating rates. This occurs due to the heat flow, since there is an endothermic first stage up to a temperature of 250 °C, and then the whole process is exothermic. This was also noticed during pyrolysis test. DSC profile during pyrolysis at low heating rate shows a completely endothermic process, but at higher heating rate, part of the process shows an exothermic behaviour, this might be due to the fact that high heating rates promotes the appearance of secondary cracking reactions of primary products.

Regarding to sample characterization, the water content is low, less than 12% for all samples, this causes a minor sensitivity of the model which might results in a deviation of the data. The samples with the highest water content are Eucalyptus bark (EB) and Eucalyptus splinters (EA).

The samples with the highest hemicellulose content, around 30%, are the Eucalyptus pellets (EP) and acacia pellets (AP), and lastly the highest percentage of hemicellulose, around 35%, appear in the Eucalyptus branch (ER). Cellulose content was higher in the samples of eucalyptus bark (EC) and splinters (EA), with an average content of 36% and 41% respectively.

The average value obtained from lignin in all samples is about 20% during pyrolysis and 30% during the combustion. Eucalyptus pellets (EP) and eucalyptus branches (ER) are the samples that shown the least amount of lignin with an average of 16% during the pyrolysis. Lignin content is highly variable since lignin decomposes over a wide temperature range and at lower heating rates there is a more efficient heat transfer, which leads to more efficient degradation of lignin.

References

- [1] P. Basu, Biomass Gasification and Pyrolysis. Practical Design., Burlington: Elsevier, 2010.
- [2] G. M. F. Shafizadeh, "Chemical composition and thermal analysis of cottonwood," Carbohydrate Research, vol. 16, no. 2, pp. 273-277, 1971.
- [3] International Energy Agency (IEA), "Technology Roadmap: Bioenergy for Heat and Power," 2012.
- [4] The International Renewable Energy Agency (IRENA), "Renewable Energy Statistics," Abu Dhabi, 2017.
- [5] International Renewable Energy Agency (IRENA), "Biomass for power generation," vol. 1, no. 1/5, June 2012.
- [6] International Energy Agency (IEA), "World Energy Outlook," 2013.
- [7] International Energy Agency (IEA) and Food and Agriculture Organization, "How2Guide for Bioenergy," 2017.
- [8] United Nations Framework Convention on Climate Change, "Clarifications on definition of biomass and consideration of changes in carbon pools due to a CDM project activity," Bonn, Germany, 8 July 2005.
- [9] Z. Anwar, M. Gulfranz and M. Irshad, "Agro-industrial lignocellulosic biomass a key to unlock the future bio-energy: A brief review," Journal of Radiation Research and Applied Sciences, vol. 7, no. 2, pp. 163-173, April 2014.
- [10] A. Sullivan and R. Ball, "Thermal decomposition and combustion chemistry of cellulosic biomass," Atmospheric Environment, vol. 47, pp. 133-141, February 2012.
- [11] E. Sjöström, Wood Chemistry: Fundamentals and Applications, Espoo, Finland: Academic Press, 1993.
- [12] M. Poletto and H. L. Ornaghi Junior, Cellulose - Fundamental Aspects and Current Trends, InTech, December 2009.
- [13] E. Z. Lincoln Taiz, Fisiología vegetal volumen I, Catelló de la Plana: Universitat Jaume I, D.L., 2006.
- [14] H. Goyal, D. Seal and R. Saxena, "Bio-fuels from thermochemical conversion of renewable resources: A review," Renewable & sustainable energy reviews , vol. 12, pp. 504-517, 2008.
- [15] L. Xu, Y. Jiang and L. Wang, "Thermal decomposition of rape straw: Pyrolysis modeling and kinetic study via particle swarm optimization," Energy Conversion and Management , vol. 146, pp. 124-133, 2017.
- [16] K. Werner, L. Pommer and M. Broström, "Thermal decomposition of hemicelluloses," Journal of Analytical and Applied Pyrolysis, vol. 110, pp. 130-137, 2014.
- [17] A. Bridgwater, "Renewable fuels and chemicals by thermal processing of biomass," Chemical Engineering Journal, vol. 91, pp. 87-102, 2003.
- [18] A. Gómez, W. Klose and S. Rincón , "Pirólisis de biomasa. Cuesco de Palma," Kassel University Press, Kassel, Alemania, 2008.
- [19] Y. Haiping , Y. Rong , C. Hanping and Z. Chuguang, "Characteristics of hemicellulose, cellulose and lignin pyrolysis," vol. Fuel 2007, no. 86, 2006.

- [20] T. Mani, P. Murugan and J. Abedi, "Pyrolysis of wheat straw in a thermogravimetric analyzer: Effect of particle size and heating rate on devolatilization and estimation of global kinetics," *Chemical Engineering Research and Design*, vol. 88, p. 952–958, 2010.
- [21] N. P. Niemelä, H. Tolvanen and T. Saarinen, "CFD based reactivity parameter determination for biomass particles of multiple size ranges in high heating rate devolatilization," *Energy*, pp. 676-687, 2017.
- [22] J.-E. Joubert, "Pyrolysis of *Eucalyptus grandis*," Stellenbosch University, 2013.
- [23] D. Chen, Y. Li, K. Cen, M. Luo, H. Li and B. Lu, "Pyrolysis polygeneration of poplar wood: Effect of heating rate and pyrolysis temperature," *Bioresource Technology*, vol. 218, p. 780–788, 2016.
- [24] N. Prakash and T. Karunanithi, "Kinetic Modeling in Biomass Pyrolysis – A Review," *Journal of Applied Sciences Research*, vol. 4, pp. 1627-1636, 2008.
- [25] K. Min, "Vapor-phase Thermal Analysis of Pyrolysis Products," *COMBUSTION AND FLAME*, vol. 30, pp. 285-294, 1977.
- [26] C. Vovelle, H. Mellottié and R. Delbourgo, "Kinetics of the thermal degradation of cellulose and wood in inert and oxidative atmospheres," *Nineteenth Symposium (International) on Combustion*, pp. 797-805, 1982.
- [27] G. Varhegyi and M. J. Antal, "Kinetics of the Thermal Decomposition of Cellulose, Hemicellulose, and Sugar Cane Bagasse," *Energy & Fuels*, vol. 3, pp. 329-335, 1989.
- [28] F. Kilzer and A. Broido, "Speculations on the nature of cellulose pyrolysis," *Pyrodynamics*, vol. 2, pp. 151-163, 1965.
- [29] A. G. W. Bradbury, Y. Sakai and F. Shafizadeh, "A Kinetic Model for Pyrolysis of Cellulose," *Journal of Applied Polymer Science*, vol. 23, pp. 3271-3280, 1979.
- [30] A. Broido and M. A. Nelson, "Char Yield on Pyrolysis of Cellulose," *COMBUSTION AND FLAME*, vol. 24, pp. 263-268, 1975.
- [31] M. G. Grønli, "A theoretical and experimental study of the thermal degradation of biomass," Trondheim, Norway, 1996.
- [32] P. K. Chatterjee and C. M. Conrad, "Kinetics of the Pyrolysis of Cotton Cellulose," *Textile Research Journal*, vol. 36, no. 6, 1966.
- [33] C. A. Koufopoulos, A. Lucchesi and G. Maschio, "Kinetic modelling of the pyrolysis of biomass and biomass components," *The Canadian Journal of Chemical Engineering*, vol. 67, no. 1, 1989.
- [34] C. D. Blasi, "Comparison of semi-global mechanisms for primary pyrolysis of lignocellulosic fuels," *Journal of Analytical and Applied Pyrolysis*, vol. 47, p. 43–64, 1998.
- [35] A. Anca-Couce, "Reaction mechanisms and multi-scale modelling of lignocellulosic," *Progress in Energy and Combustion Science*, vol. 53, pp. 41-79, 2015.
- [36] S. Vyazovkin, K. Chrissafis and M. L. Di Lorenzo, "ICTAC Kinetics Committee recommendations for collecting," *Thermochemica Acta*, vol. 590, p. 1–23, 2014.
- [37] D. Trache, A. Abdelaziz and B. Siouani, "A simple and linear isoconversional method to determine the pre-exponential factors and the mathematical reaction mechanism functions," *Journal of Thermal Analysis and Calorimetry*, vol. 128, pp. 335-348, 2016.
- [38] T. Ozawa, "A new method of analyzing thermogravimetric data," *Bull. Chem. Soc. Jpn.*, vol. 38, pp. 1881-1886, 1965.

- [39] J. H. Flynn and L. A. Wall, "General treatment of the thermogravimetric of polymers," *J. Res. Natl. Bur. Stand. A*, vol. 70, pp. 487-523, 1966.
- [40] S. Wang, G. Dai, H. Yang and Z. Luo, "Lignocellulosic biomass pyrolysis mechanism: A state-of-the-art review," *Progress in Energy and Combustion Science*, vol. 62, pp. 33-86, 2017.
- [41] T. Akahira and T. Sunose, "Joint convention of four electrical institutes," *Res. Report CHIBA Inst. Technol.*, vol. 16, pp. 22-31, 1971.
- [42] S. V. Vyazovkin and A. I. Lesnikovich, "Estimation of the pre-exponential factor in the isoconversional calculation of effective kinetic parameters," *Thermochimica Acta*, vol. 128, pp. 297-300, 1988.
- [43] L. N. Samuelsson, *Isoconversional analysis for the prediction of mass-loss rates during pyrolysis of biomass*, Stockholm, Sweden, 2016.
- [44] Y. Haiping , Y. Rong , Z. Chuguang and H. L. Dong , "In-Depth Investigation of Biomass Pyrolysis Based on Three Major Components: Hemicellulose, Cellulose and Lignin," *Energy & Fuels*, vol. 20, pp. 388-393, 2006.
- [45] M. Brebu and V. Cornelia , "Thermal degradation of lignin- A review," *Cellulose Chemistry and Technology*, pp. 353-363, 2009.
- [46] M. V. Kok and E. Özgür, "Thermal analysis and kinetics of biomass samples," *Fuel Processing Technology*, p. 739-743, 2013.
- [47] Z. Chen, Q. Zhu, X. Wang, B. Xiao and S. Liu, "Pyrolysis behaviors and kinetic studies on Eucalyptus residues using thermogravimetric analysis," *Energy Conversion and Management*, vol. 105, pp. 251-259, 2015.
- [48] A. Heidari, R. S. Stahl, H. Younesi, A. Rashidi, N. Troeger and A. A. Ghoreyshi, "Effect of process conditions on product yield and composition of fast pyrolysis of Eucalyptus grandis in fluidized bed reactor," *Journal of Industrial and Engineering Chemistry*, vol. 20, p. 2594-2602, 2013.